Mestrado Integrado em Engenharia Química

Steel reinforcement for tires - Test method development to assess the adhesion of steel reinforcements to rubber under dynamic conditions

Master Thesis

By

José Manuel Silva Almeida

performed at

Continental AG - Body Compound & Reinforcement Technology Department

Supervisor at FEUP: **Prof. Fernão Magalhães**

Supervisor at Continental: **Dr. Thomas Kramer**

Departamento de Engenharia Química

July of 2016

Acknowledgements

These last months have been a great professional and personal experience, it has been truly a test living in a foreign country, dealing with daily challenges and projects in the company and putting in practice all that I learned in the last 5 years.

I'd like to start by thanking Dr. Thomas Kramer for giving this opportunity for young students to develop their professional experience, for all the early and weekly meetings, all the support and help provided for the progress of my work and all the effort to make my work easier, faster and more challenging.

A special thanks to Prof. Fernão Magalhães for his availability and interest to be my supervisor despite that it's quite difficult to guide and help a thesis from so far.

I'd also like to thank Mr. Thomas Felten, Tiago Moura, Mr. Claus Stark and Christian Neufeld for all the support given throughout my thesis and work progress in the company.

A big thanks to everyone who helped me incorporate into the continental family on the department of Body & Compound Reinforcement Technology: Christoph Eichhorst, Claudia Grote, Daniel Mohr, Jakob Hey, Joe Guardalabene, Michael Schunack, Miguel Bispo, Nermeen Nabih, Ute Poehler, Virpin Rajan and all the workers over on the Laboratory of Reinforcement materials.

I'd also like to thank everyone who help and support me, even if they're not geographically close, my parents Jorge and Fátima Almeida, my sister Ana Almeida, Marek Mannes, Prof. Luís Madeira, my friends back from university and Czech Republic and the other interns from Continental that I got the change to meet and develop a friendship with.

Finally I'd like to thank and dedicate this work to my close friend Júnio Ribeiro who believed in me every time I didn't, that encouraged me to study abroad and to apply for this position.

Resumo

O foco deste trabalho consistiu em determinar as melhores condições padrão para realizar um teste dinâmico, de escala laboratorial, capaz de alcançar resultados de adesão satisfatórios entre as cordas de aço e a matriz de borracha, que correspondam às condições reais dos pneus usando os métodos: *Dynamic T-Test* e *3-Cord Adhesion Test*. Um objetivo suplementar nesta tese foi utilizando um método de reforços têxteis (*Green Adhesion Test*), avaliar se o uso de diferentes construções das amostras levaria a resultados que se podessem relacionar com os resultados fornecidos pela planta de Lousado em Portugal.

Para os testes de reforço de aço as condições padrão ideais foram: um envelhecimento de 5 dias sob vapor e uma fadiga a 80 °C com uma amplitude de 10 mm e 1,00 milhões de ciclos para o *3-Cord Adhesion Test* e um envelhecimento de 5 dias sob vapor e uma fadiga a 80 °C durante 1,00 milhões de ciclos para o *Dynamic T-Test*. Nestas condições a redução da força foi de 72.75 ± 4.62 % e 43.56 ± 4.98 %, respetivamente.

Para ambos os métodos, concluiu-se que os testes à temperatura ambiente não podem ser considerados para a avaliação do desempenho do composto e que ambos apresentam vantagens económicas e no consumo de tempo para a empresa quando comparados com o teste padrão atualmente usado (*Drum-test*).

Os resultados do *Green Adhesion Test* mostraram que, para as diferentes construções de amostras utilizadas, houve uma redução homogénea da força. O teste utilizando corda calandrada teve uma redução de 63.4 ± 5.1 % e a utilização de corda não calandrada uma redução de 33.5 ± 2.3 %. Isto permitiu concluir que estas diferentes construções da amostra podem ser usadas para futuros estudos sobre as capacidades de adesão de reforços têxteis na borracha utilizando material não vulcanizado.

Palavras-chave: reforços; adesão; fadiga; ensaio dinâmico.

Abstract

The focus of this thesis was to determine the best standard conditions to perform a laboratory-scale dynamic test able to achieve satisfactory results of the adhesion between steel cord and the rubber matrix, matching the tire's real conditions, using a less time consuming test: Dynamic T-Test and 3-Cord Test. An additional goal for this thesis regards a textile reinforcement test method (Green Adhesion test), was to evaluate if the use of different sample constructions would lead to results that could be compared with the standard results provided from the Lousado plant in Portugal.

For the steel reinforcement test methods, the best standard conditions were: an aging condition of 5 days under Steam and a fatigue at 80 °C with an amplitude of 10 mm and 1.00 million cycles for the 3-Cord adhesion test and an aging condition of 5 days under Steam and a fatigue at 80 °C during 1.00 million cycles for the Dynamic t-test. In these conditions the final reduction of the pull-out-force was 72.75 ± 4.62 % and 43.56 ± 4.98 %, respectively.

For both methods, it was concluded that the measurements at room temperature cannot be considered for the studies of the composite's performance and that both tests showed a time and financial advantage for the company when compared with the current standard test used (Drum-test).

The results on the Green adhesion showed that, for each sample construction configuration, there was a homogeneous reduction. The test using dipped cord got a reduction of 63.4 ± 5.1 % and the use of calendered cord of 33.5 ± 2.3 %. This allowed concluding that these sample constructions can be used for further studies of the adhesion capabilities of textile reinforcements in rubber using non-vulcanized material.

Keywords: reinforcements; adhesion; fatigue; dynamic test.

Official Statement

I declare, under honor commitment, that the present work is original and that every non original contribution was properly referred, by identifying its source.

Index

Acknowledgements iii

Resumo v

Abstract vii

Official Statement ix

Index xi

Index of Figures xv

Index of Tables xix

Notation and Glossary xxi

List of variables xxi

List of acronyms xxi

1 Introduction 1

1.1 Project presentation and framework 1

1.2 Continental AG 1

1.3 Work goals and contributions 2

1.4 Thesis Organization 2

2 State of art 5

2.1 Tires 5

2.1.1 Components 5

2.1.2 Composition 6

2.1.3 Types 6

2.2 Tire reinforcement 7

2.2.1 Reinforcement materials 8

2.2.2 Steel reinforcement and Steel Cord 9

2.3 Tire Cord Adhesion 10

2.3.1 Mechanism of rubber-brass bonding 11

2.3.2 Vulcanization process 11

2.3.3 Aging of the rubber-brass bond 12

3 Testing methods 15

3.1 Methods of dynamic adhesion testing 15
3.1.1 Tension test methods 15
3.1.2 Compression test methods 15
3.1.3 Flexing test methods 16
3.2 Adhesion Reinforcement test methods 16
3.2.1 Green Adhesion Test 16
3.2.2 3-Cord Adhesion Test 17
3.2.3 Dynamic T-Test 19
3.3 Aging and Fatigue conditioning 23
3.4 Equipment 25
3.4.1 Frank Machine 25
3.4.2 Zwick Tensile Tester 26
3.4.3 MTS machine 26
4 Results and discussion 29
4.1 Green Adhesion Test 29
4.2 3-Cord Adhesion Test 31
4.3 Dynamic T-Test 40
4.4 3-Cord Adhesion Test Vs Dynamic T-Test 43
5 Conclusions 45
6 Project Assessment 47
6.1 Achieved goals 47
6.2 Additional projects 47
6.3 Limitations and Future Work 47
6.4 Final Assessment 48
References 49
Appendix A – Sample preparation 51
Appendix A.1 – Green adhesion sample preparation 51
Appendix A.2 – 3-Cord Adhesion sample preparation 52
Appendix A.3 – Dynamic T-Test sample preparation 54

Appendix B – Lab test results 56

Appendix B.1 – Green Adhesion Test 56

Appendix B.2 – 3-Cord Adhesion Test 57

Appendix B.2.1 – Influence of the Sample's thickness 57

Appendix B.2.2 – Influence of the test starting position 58

Appendix B.2.3 – Reproducibility of the results 59

Appendix B.2.4 – Determine the best standard conditions 61

Appendix B.3 – Dynamic T-Test 66

Index of Figures

Figure 2. 1 - Radial tire's structure (source: Continental AG, 2008) 6

Figure 2. 2 - Structure of a bias tire (on the left) and of a radial tire (on the right) (source: Hankook Tire) 7

Figure 2. 3 - Components that incorporate tire cord reinforcements (source: Thomas Kramer, 2015) ... 8

Figure 2. 4 - Representation of the Steel cord composition (source: U.S. Department of Transportation, 2006) 10

Figure 2. 5 - Diagram of a brass-coated steel cord surface before vulcanization (a) and after (b) (source: W. Stephen Fulton, 2004) 12

Figure 2. 6 - Interfacial structures formed after aging of the rubber-metal bond (source: W. Stephen Fulton, 2004) 12

Figure 2. 7 - Mechanisms of deterioration of adhesion due to the presence of moisture (source: U.S. Department of Transportation, 2006) 13

Figure 3. 1 - Illustration of the Green Adhesion Test 17

Figure 3. 2 - Illustration of the 3-Cord Adhesion Test (source: Thomas Felten, 2016) 18

Figure 3. 3 - Conditions set for the 3-Cord Adhesion Test study 19

Figure 3. 4 - Graphic illustration of the increase of the force during the Dynamic T-Test (source: Thomas Felten, 2016) 20

Figure 3. 5 - Measurement of Dynamic stiffness and phase lag (source: Frampton, 2009) 20

Figure 3. 6 - Phase lag between stress and strain (source: Guelho, Reis, & Fontul, 2012) 21

Figure 3. 7 - Illustration of the Dynamic T-Test (source: Thomas Felten, 2016) 22

Figure 3. 8 - Illustration of the sample before and after the test procedure (source: Arup K. Chandra, R. Mukhopadhyay, 1996) 22

Figure 3. 9 - Conditions set for the Dynamic T-Test study 23

Figure 3. 10 - Container and Oven used for the Steam Conditioning 23

Figure 3. 11 - Illustration of fatigue on 3-Cord Adhesion (a) and Dynamic T-test samples (b) (source: Thomas Felten, 2016) 24

Figure 3. 12 - Graphic illustration of the displacement during the fatigue procedure (source: Thomas Felten, 2016) 24

Figure 3. 13 - Evolution of the force during the fatigue procedure 25

Figure 3. 14 - Frank Machine (source: Thomas Felten, 2016) 26

Figure 3. 15 - Zwick Tensile Tester (a), clamps for the Green Adhesion (b) and for the 3-Cord Test (c) (source: The Zwick Roell) *26*

Figure 3. 16 - MTS Machine, clamps for the 3-Cord Test (b) and for the Dynamic T-Test (c) (source: MTS Systems Corporation) *27*

Figure 4. 1 - Test results from the new sample construction configuration and the standard results .. *29*

Figure 4. 2 - Relation of the green adhesion with the cord thickness for the different materials and sample constructions *30*

Figure 4. 3 - Decreasing of the green adhesion for the test specimens *31*

Figure 4. 4 - Graphic representation of a desired and an undesired result for the 3-Cord adhesion test *32*

Figure 4. 5 - Illustration of the different set conditions to perform the test *33*

Figure 4. 6 - Evaluation of the deviation for the different test throughout the test procedure *34*

Figure 4. 7 -Test results for the different samples *34*

Figure 4. 8 - Set conditions of the sample to perform the 3-Cord adhesion test *35*

Figure 4. 9 - Illustration of the friction occurrence during the test procedure *35*

Figure 4. 10 - Test results from experiment 1 and experiment 5 ..... *36*

Figure 4. 11 - Test results from experiment 8 and experiment 9 ..... *36*

Figure 4. 12 - Samples from experiment 3 after fatigue *37*

Figure 4. 13 - Samples from experiment 4 after fatigue *37*

Figure 4. 14 - Test results from experiment 8 and experiment 9 ..... *38*

Figure 4. 15 - Test results from experiment 10 and experiment 11 ..... *39*

Figure 4. 16 - Test results from experiment 6 and experiment 7 ..... *39*

Figure 4. 17 - Test results from two different samples for experiment 1 ..... *40*

Figure 4. 18 - Evolution of the number of cycles and pull-out-force on experiment 3 ..... *41*

Figure 4. 19 - Evolution of the number of cycles and pull-out-force on experiment 5 ..... *41*

Figure 4. 20 - Evolution of the number of cycles and pull-out-force on experiment 2 ..... *42*

Figure 4. 21 - Evolution of the number of cycles and pull-out-force on experiment 4 ..... *42*

Figure 4. 22 - Evolution of the number of cycles and pull-out-force on experiment 6 ..... *42*

Figure A. 1 - Dimension of the strips and sample construction of the complete specimen (source: Burghof, 2015) *51*

Figure A. 2 - Illustration of the different sample contractions: calendered fabric (a); calendered cords; dipped cords (c) *52*

Figure A. 3 - Example of prepared sample for testing *52*

Figure A. 4 - Illustration of the angle formed by the to layers when combined together (source: Thomas Felten, 2016) *53*

Figure A. 5 - Mould used to prepare the 3-Cord Adhesion samples *53*

Figure A. 6 - 3-Cord Adhesion sample fresh (a); after aging condition (b); after fatigue (c) *54*

Figure A. 7 - Mould used to prepare the Dynamic T-Test samples *54*

Figure A. 8 - Dynamic T-Test sample fresh (a); after aging condition (b); after fatigue (c) *55*

Figure B. 1 - Graphic representation of the test results *57*

Figure B. 2 - Graphic representation of the modified test results *58*

Figure B. 3 - Graphic representation of the standard force on the first test *58*

Figure B. 4 - Graphic representation of the standard force on the second test *59*

Figure B. 5 - Graphic representation of the standard force on the third test *59*

Figure B. 6 - Graphic representation of the standard force on the first sample *60*

Figure B. 7 - Graphic representation of the standard force on the second sample *60*

Figure B. 8 - Graphic representation of the standard force on the third sample *60*

Figure B. 9 - Graphic representation of the standard force for the experiment 1 ..... *61*

Figure B. 10 – Graphic representation of the standard force for the experiment 2 ..... *61*

Figure B. 11 - Graphic representation of the standard force for the experiment 3 ..... *62*

Figure B. 12 – Graphic representation of the standard force for the experiment 4 ..... *62*

Figure B. 13 - Graphic representation of the standard force for the experiment 5 ..... *63*

Figure B. 14 – Graphic representation of the standard force for the experiment 6 ..... *63*

Figure B. 15 - Graphic representation of the standard force for the experiment 7 ..... *64*

Figure B. 16 – Graphic representation of the standard force for the experiment 8 ..... *64*

Figure B. 17 - Graphic representation of the standard force for the experiment 9 ..... *65*

Figure B. 18 – Graphic representation of the standard force for the experiment 10 ..... *65*

Figure B. 19 – Graphic representation of the standard force for the experiment 11 ..... *66*

Figure B. 20 - Test results from previous tests (Experiment 1) *66*

Figure B. 21 - Graphic illustration of the phase lag on the experiment 2 ..... *68*

Figure B. 22 - Graphic illustration of the complex dynamic stiffness on the experiment 2 68

Figure B. 23 - Graphic illustration of the phase lag on the experiment 3 69

Figure B. 24 - Graphic illustration of the complex dynamic stiffness on the experiment 3 69

Figure B. 25 - Graphic illustration of the phase lag on the experiment 4 70

Figure B. 26 - Graphic illustration of the complex dynamic stiffness on the experiment 4 70

Figure B. 27 - Graphic illustration of the phase lag on the experiment 5 71

Figure B. 28 - Graphic illustration of the complex dynamic stiffness on the experiment 5 71

Figure B. 29 - Graphic illustration of the phase lag on the experiment 6 72

Figure B. 30 - Graphic illustration of the complex dynamic stiffness on the experiment 6 72

Index of Tables

Table 4. 1 - Properties of the test specimens *29*

Table 4. 2 -Test results of the highest and lowest pull-out force *32*

Table 4. 3 - Test result deviations for the first and second test *33*

Table 4. 4 - Differences and similarities between the 3-Cord Adhesion Test and Dynamic T-Test *43*

Table B. 1 - Test results from the green adhesion test *56*

Table B. 2 - Thickness's values measured on different points of the sample *57*

Table B. 3 - Test results from the dynamic t-test *67*

Notation and Glossary

List of variables

A	Amplitude	mm
d	Thickness	mm
f	Frequency	Hz
GA	Green Adhesion	N
K*	Complex Dynamic Stiffness	N/mm
T	Period	s
δ	Phase lag	º
ΔF	Variations of force	N
Δt	Time difference between waveforms	s
Δx	Displacement	mm

List of acronyms

AG	Aktiengesellschaft
CVT	Commercial Vehicle Tires
EU	European Union
ORT	Off-the-road
PET	Polyethylene Terephthalate
PLT	Light truck tires
RF	Resorcinol Formaldehyde
TCAT	Tire cord adhesion test

1 Introduction

1.1 Project presentation and framework

Most practical rubber products include the concept of reinforcing the rubber matrix with some reinforcing agent because they are too weak to be used without these systems. There are two main possible reinforcing principles: either the rubber matrix is compounded with reinforcing fillers or the product is provided with some fiber consisting components applied in the product assembly phases.

The primary function of reinforcing is to improve the mechanical properties of the rubber compound and to give adequate functional properties to the product. In both cases it is crucially important that the additional components of rubber compound and the product are well bonded to the rubber segments of the matrix.

In the context of the properties of reinforcing fibers, there's a particular attention given to the aspects of adhesion, adhesive treatments and processing and the assessment of adhesion. The basic technology of steel based fibers and the processes used in preparing these components must achieve the optimum reinforcement and performance for a particular application (NOKIAN TYRES PLC, 2008).

Therefore, a large number of tests have been developed over the years to help in the evaluation of the adhesion strength when preformed in dynamic conditions incorporating the effect of various parameters such as cord embedment length, number of extension cycles, degree of extension, aerobic ageing, thermal ageing and compound hardness (Chandra & Mukhopadhyay, 1995). The main goal of this master's thesis is to create new testing conditions for a dynamic adhesion fatigue test method capable of providing valid results in a shorter amount of time when compared to current tests that are used now.

1.2 Continental AG

Continental was founded in Hanover in 1871 as the stock corporation "Continental-Caoutchouc und Gutta-Percha Compagnie". The company used to produce soft rubber products, rubberized fabrics and solid tires for carriages and bicycles (Continental AG, 2016).

Nowadays, Continental AG is a global automotive supplier, tire manufacturer and industrial partner to other industries. Continental ranks among the top 5 automotive suppliers worldwide as a supplier of brake systems, systems and components for powertrains and chassis, instrumentation, infotainment solutions, vehicle electronics, tires and technical elastomers,

Continental also contributes to enhanced driving safety and global climate protection (Continental AG, 2016).

Continental operates through six segments: Chassis & Safety, Powertrain, Interior, Tires, ContiTech and Other/consolidation. The Chassis & Safety segment focuses on technologies for active and passive safety and for vehicle dynamics. The Powertrain segment integrates system solutions for powertrains in vehicles of various classes. The Interior segment specializes in information management in vehicles. The Tires segment offers a range of tires, from tires for cars, trucks and buses to specialist products for construction and industrial vehicles to tires for bicycles and motorcycles. The ContiTech segment combines Continental's rubber and plastics activities for various industries. The Other/consolidation segment consists of centrally managed subsidiaries and affiliates, as well as the holding function of Continental and certain effects of consolidation (Reuters, 2016).

1.3 Work goals and contributions

The focus of this thesis was to develop a test method able to evaluate the adhesion capabilities of steel reinforcements in rubber under dynamic conditions. The need for this study can be justified by two reasons: the first one is that in the near future, compounds such as resorcinol, Cobalt and Formaldehyde may be excluded, by law of the EU, for the production of tires and the second reason is that the main test method used at the moment is the drum test, which consumes a big amount of time and material and is highly expensive.

Therefore, the objective of this thesis is to determine the best standard conditions to perform the laboratory-scale dynamic test on the samples of reference material containing the new desired composition (new compounds with reduced incorporation of resorcinol) able to achieve results that match the tire real condition, using a less time consuming test such as the Dynamic t-test and the 3-Cord test.

Another project later included in the thesis regards a textile reinforcement test method, named Green Adhesion test. The focus of this test is to evaluate the adhesion capabilities of textile reinforcements in rubber using non-vulcanized material. The goal of this study was to evaluate if using different sample constructions would lead to results that could be compared with the standard results provided from the Lousado plant in Portugal.

1.4 Thesis Organization

This thesis is organized in 6 chapters, being each of them outlined on the next paragraphs:

Chapter 1, Introduction gives an initial approach to automotive industries market, with an important reference to Continental AG role on global tire market and the most important aspects regarding tire reinforcement;

Chapter 2, State of the Art is a deeper introduction to tires technology and engineering. Furthermore, it explores the topics such as steel reinforcement and cord to rubber adhesion mechanisms;

Chapter 3, Testing methods explains the methodology used for both textile and steel reinforcement dynamic tests, the sample construction procedure and explore the procedure, equipments and test conditions for each method;

Chapter 4, Results and discussion reviews all the experimental work results, its discussion based on literature and external contributions and determines the most suitable conditions for each method;

Chapter 5, Conclusions points out all the main aspects strongly sustained by this work;

Chapter 6, Bibliography is a complete list of all the references used throughout this work.

2 State of art

2.1 Tires

Tires are highly engineered structural composites whose performance can be designed to meet the vehicle manufacturer's ride, handling and traction criteria, plus the quality and performance expectations of the customer.

Historically, pneumatic tires began in Great Britain during the late 1800s as an upgrade from solid rubber tires principally produced for bicycle applications. Larger tires were introduced in the early 1920s with applications in the motor vehicle industry. In the late 1960s belted bias tires became popular and radial tires, first introduced in Europe, became popular in the USA starting in the early 1970s and now dominate the passenger tire market (Brewer, Clark, & Gent, February 2006).

The primary functions of the tires are to provide the interface between the vehicle and the highway, to support the vehicle's load, ensure the transmission of driving and braking forces and the directional stability of the vehicle, to deal with the complex effects of weather conditions and to absorb road irregularities (Omark, 2014).

2.1.1 Components

Every modern passenger car tire has a complex structure containing several components (fig. 2.1) that can be divided into three main parts:

- **Tread** (1) - Consists on a thick layer that comes into direct contact with the road surface, highly resistant to fracture in order to protect the carcass and belt located in the tire's interior;
- **Belt** – Strong reinforcement layer located in the circumference between the tread and the carcass. It absorbs external shock, prevents splintering or injury and also reinforces the strength of the tread (Hankook Tire, 2016). The belt includes:
    - **Jointless cap plies** (2) that enable high speeds and **Steel-cord belt plies** (3) which optimize directional stability and rolling resistance.
- **Carcass** – It's the framework of the tire, includes all layers made up of tire cord and absorbs the tire's internal air pressure, weight and shock. The carcass includes:
    - The **Textile cord ply** (4) that control internal pressure and maintains the tire's shape, the **Inner liner** (5) that makes the tire airtight, a **Side wall** (6) which protects from external damage, a **Bead core** (9) that ensure firm seating on the rim and a **Bead reinforcement** (7) and a **Bead apex** (8) that promote directional and directional stability (Continental AG, 2008).

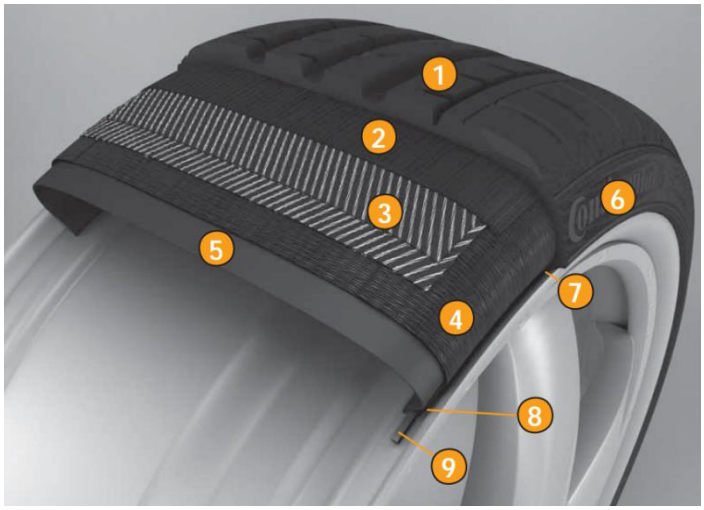

Figure 2. 1 - Radial tire's structure (source: Continental AG, 2008)

2.1.2 Composition

A typical car tire uses about 60 raw materials and there are more than a dozen specially formulated compounds used in the interior of the tire. The main components present in a tire are:

- **Polymers** - Described as the backbone of rubber compounds, they consist of natural or synthetic rubber;
- **Reinforcing Fillers** – Fillers such as carbon black and silica are used to give strength and longevity to the tire (Cinaralp & Zullo, 2012);
- **Softeners** - Softeners like petroleum oils, resins and waxes are principally used to improve the stickiness of the non-vulcanized compounds;
- **Anti-degradants** - Waxes, antioxidants, and antiozonants are added to rubber compounds to help protect tires against deterioration by ozone, oxygen and heat.
- **Curatives** - Allow the polymer chains to become linked during vulcanization or curing, transforming the viscous compounds into strong elastic materials (Brewer, Clark, & Gent, February 2006).

2.1.3 Types

There are many different types of tires. Tread pattern and rubber compound varies significantly between tires for different purposes, for example summer or winter use. Choosing the right tires can improve the vehicle handling, increase the safety and reduce wear significantly.

Tires can be generally classified according to their structure as bias tires and radial tires (fig. 2.2). The bias tires have body ply cords that are laid at angles substantially less than 90º to the tread centerline and have a simple construction and easy to produce and the radial tires have body ply cords that are laid radially from bead to bead at 90º to the centerline of the tread to add strength and stability (Brewer, Clark, & Gent, February 2006).

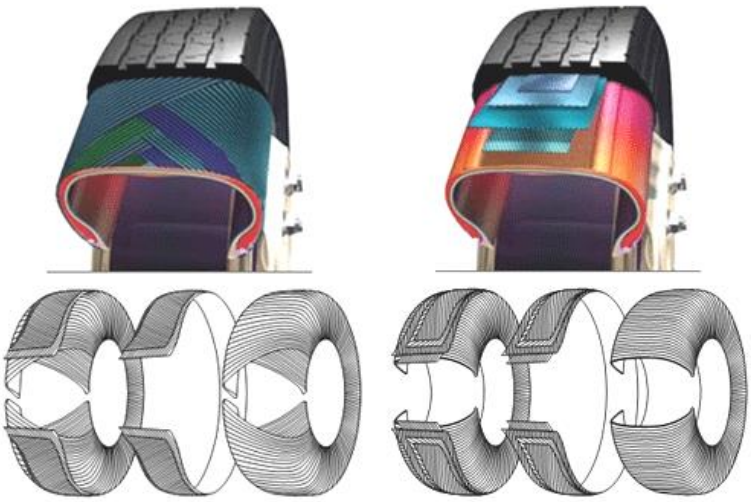

Figure 2. 2 - Structure of a bias tire (left) and of a radial tire (right) (source: Hankook Tire)

2.2 Tire reinforcement

The reinforcement on tire is ensured by the use of tire cords. Tire cords are the strength elements the tire, it defines its shape, supports the loads and contains the inflation gas. Cords provide the axial and lateral rigidity for acceleration, braking and cornering and dimensional stability for uniformity, handling and ride. Cords also provide fatigue, bruise and resistance to separation for durability (NOKIAN TYRES PLC, 2008). The cord requirements are:

- High axial orientation for axial stiffness and strength (high modulus in tension);
- Good lateral flexibility (low modulus in bending);
- Filaments with high length to diameter ratio and tensile strength;
- Filaments twisted into cords to function as a unit and exert axial strength;
- Twist and tire design to prevent cord from operating in compression.

The reinforcements can be divided into two groups depending on the material, ideal cord properties and components of the tire where they'll be used: Textile and Steel reinforcement (fig. 2.3).

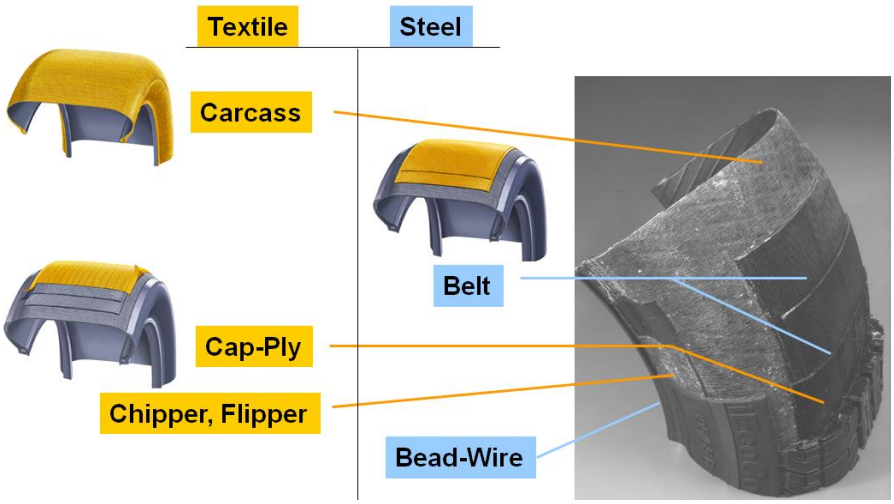

Figure 2. 3 - Components that incorporate tire cord reinforcements (source: Thomas Kramer, 2015)

2.2.1 Reinforcement materials

There are several types of reinforcement materials that may be used depending on the usage meant for the car (Brewer, Clark, & Gent, February 2006):

- **Nylon** are synthetic long chain polymers produced by continuous polymerization/spinning or melt spinning commonly used in radial passenger tire's cap, overlay ply and belt edge cap strip material;
- **PET** tire cords are also synthetic, long chain polymers produced by continuous polymerization/spinning or melt spinning and are commonly used in radial body plies with some limited applications as belt plies;
- **Rayon** is a body ply cord or belt reinforcement made from cellulose produced by wet spinning;
- **Aramid** is a synthetic, high tenacity organic fiber produced by solvent spinning, 2 to 3 times stronger than PET and nylon and it can be used for belt or stabilizer ply material as a light weight alternative to steel cord;
- **Steel cord** is a carbon steel wire coated with brass that has been drawn, plated, twisted and wound into multiple-filament bundles and it's the principal belt ply material used in radial passenger tires;
- **Bead wire** is carbon steel wire coated with bronze that has been produced by drawing and plating. Filaments are wound into two hoops, one on each side of the tire, in various configurations that serve to anchor the inflated tire to the rim.

2.2.2 Steel reinforcement and Steel Cord

Steel reinforcements are used in the bead core and the tread in Light Truck Tires (PLT) and most Commercial Vehicle Tires (CVT), although some CVT and high performance PLT also use steel reinforcements on the sidewall or as a mesh from bead to bead (Almeida, 2012). In passenger car tires the steel cord is used in the belt, in truck radial tires is used both in the belt and in the carcass and in Off-the-road (OTR) tires it is used as a breaker for puncture protection (NOKIAN TYRES PLC, 2008).

Steel tire cord was developed almost 60 years ago and it was adopted in Europe with the improvement of the radial tire. Steel cord met the requirements for an acceptable cost, giving high strength and compression stiffness with acceptable bending stiffness, good resistance to fretting fatigue and good adhesion to rubber.

Steel is a metal alloy whose major component is iron and with carbon content between 0.02% and 1.7% by weight and the most cost effective alloying material. There's a varying the amount of alloying elements as well as steel controls qualities standards such as the hardness, elasticity, ductility and tensile strength of the resulting steel. Steel cord is stronger than fiber materials, have excellent heat resistance and fatigue resistance with no contraction.

2.2.2.1 General Characteristics

The raw material for the production of the Steel cord is wire rod and the composition of the cord may depend on the tensile strength vale. Traditionally steel tire cord has tensile strength about 2800 MPa and this type of steel cord is called normal tensile. The average steel composition of Steel cord is:

Normal tensile

- Carbon 0.725%;
- Manganese 0.525%;
- Silicon 0.230%;
- Sulphur 0.010%;
- Phosphorus 0.010%;
- Traces of copper, chromium and nickel.

High tensile

- Carbon 0.825%;
- Manganese 0.525%;
- Silicon 0.210%;
- Sulphur 0.006%;
- Phosphorus 0.008%;
- Traces of copper, chromium and nickel.

2.2.2.2 Steel Cord components

Steel cord has four basic components (fig. 2.4):

- **Filament** or **Wire** (1) - Metal fiber used as an individual element in a strand or cord. Standard filament diameters go from 0.15 to 0.38 mm;
- **Strand** (2) - Group of steel filaments twisted together;
- **Cord** (3) - Formed structure composed of two or more filaments when used as an end product or a combination of strands or filaments and strands;
- **Spiral Wrap** (4) - Spiral wrap filament wound around a steel cord to keep the cord structure together (NOKIAN TYRES PLC, 2008).

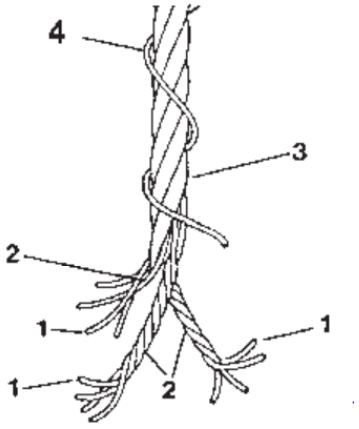

Figure 2. 4 - Representation of the Steel cord composition (source: U.S. Department of Transportation, 2006)

2.2.2.3 Steel Cord Construction Types

There are several types of cord products available based on variations in the manufacturing and twisting procedures. The most common construction types are:

Regular Cord	the direction of lay in the strands is opposite to the direction of lay in closing the cord	
Lang's Lay Cord	the direction of lay in the strands is the same as the direction of lay in closing the cord	
Open Cord	the wires are loosely associated and movable relative to each other to enable rubber to penetrate into the cord	
Compact Cord	the filaments have linear contact with each other and the strand and the cord have the same direction	

2.3 Tire Cord Adhesion

A good adhesion between brass-coated steel cord and rubber compound is essential for a long-term performance of tires. However, the rubber-metal interface is prone likely to suffer

from deterioration mainly under conditions of high humidity and salt, causing the reinforcements by steel cord to be reduce. To prevent this occurrence, various organic salts are used to improve and maintain a good bonding at the rubber-metal interface (Crowther, 2001).

2.3.1 Mechanism of rubber-brass bonding

When forming a tire cord, cooper and zinc are electro-deposited sequentially on to drawn steel wire and treated by a thermal diffusion process to produce a brass alloy coating. The produced steel cord filament coated has a brass layer of approximately 0.2 μm and with a composition of cooper of 63.5%. The adhesion force tends to a maximum value with a copper content between 67% and 72% but a better retention of adhesion after humid conditions is achieved at a lower copper content (Crowther, 2001).

When brass-coated wire is drawn during the formation process, Zn^{2+} ions diffuse to the surface and are oxidized to form a ZnO layer and also thin CuO skin. The ZnO layer also contains metallic copper inclusions formed as a result of the internal oxidation mechanism of zinc (fig. 2.5).

2.3.2 Vulcanization process

During vulcanization, the brass surface is exposed to active sulphur containing molecules and creates a strong bond between the rubber compound and the tire cord by the action of an interfacial, non-stoichiometric cooper sulfide layer that grows before the rubber is fully cross-linked. At an early stage of vulcanization, Cu^{+} and Zn^{+} ions and free electrons move to the surface of the brass wire via cationic diffusion and a Cu_xS layer, with some ZnS inclusions, is formed by a process called sulphidation. The ZnS formed initially is overgrown by Cu_xS at a later stage, which rate is sufficient to allow growth to a thickness that is essential for a good bond formation. The thickness of the Cu_xS layer is influenced by several factors, such as the copper content of the ZnS layer and the curing conditions (figure 2.5).

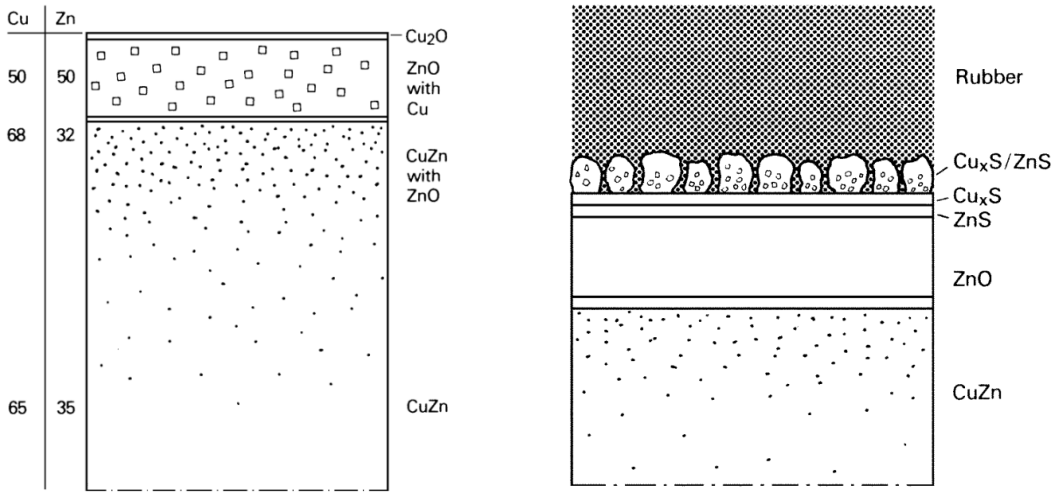

Figure 2. 5 - Diagram of a brass-coated steel cord surface before vulcanization (left) and after (right) (source: W. Stephen Fulton, 2004)

2.3.3 Aging of the rubber-brass bond

The degradation of the rubber-brass bond may be due to several processes, including heat, steam, humidity, oxygen and electrochemical corrosion. During heat aging it also occurs the deterioration of the interface. Copper migrates, by cationic diffusion, through ZnS and Cu_xS to thicken the existing Cu_xS layer which cracks and weakens the rubber-metal bond. When the Cu_xS layer stops growing, the Zn^{2+} ions diffuse through the entire interfacial layer and creates the $ZnO/Zn(OH)_2$ layer (fig. 2.6). This diffusion can be slowed down under dry conditions, but eventually $ZnO/Zn(OH)_2$ will be created on the metal surface to weaken the bond.

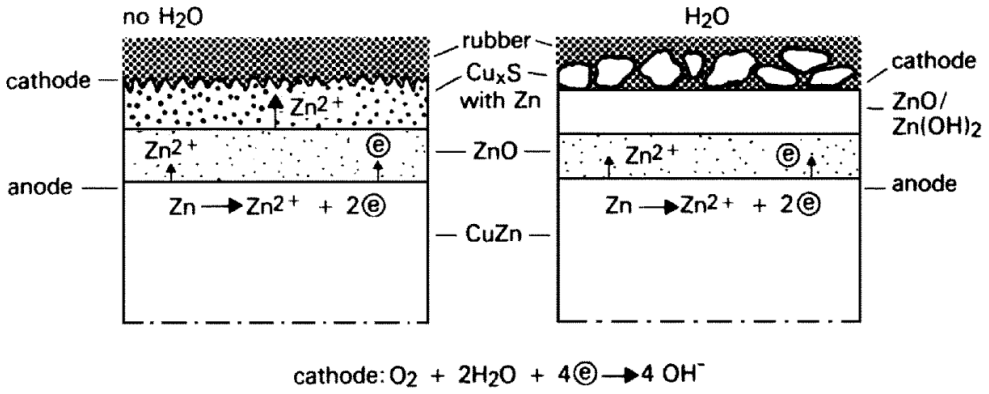

Figure 2. 6 - Interfacial structures formed after aging of the rubber-metal bond (source: W. Stephen Fulton, 2004)

The formation of the $ZnO/Zn(OH)_2$ destroys the integrity of the Cu_xS layer and debonding occurs (Dezincification). Brass plated steel cord that contains low levels of cooper is not so

sensitive to decohesion caused by moisture and compounding with high levels of ZnO also helps to inhibit the dezincification by reducing the diffusion of the Zn^{2+} ions (Crowther, 2001).

Bond durability is tested by measuring bond strength after various aging times such as: Dry heat aging, steam aging, aging in high humidity and salt bath immersion. The rubber coverage of the wire after testing is regarded as equally important as the retained bond strength of the rubber compound. Corrosion of steel can destroy both the adhesive bond and the wire itself, figure 2.7 shows a view of moisture attack on wire through galvanic action if the brass coating is damaged or if water can wick into the cord interstices (Brewer, Clark, & Gent, February 2006).

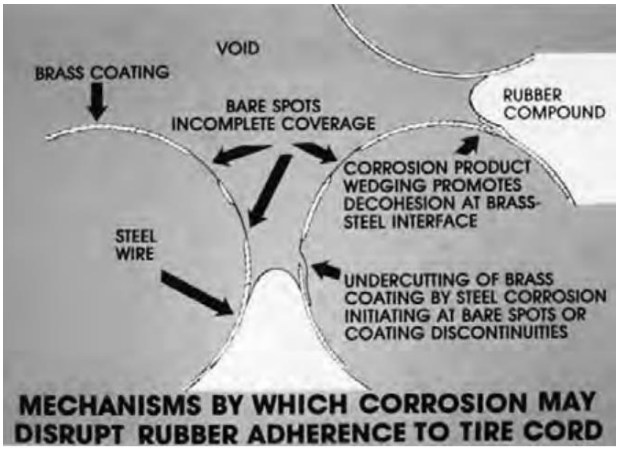

Figure 2. 7 - Mechanisms of deterioration of adhesion due to the presence of moisture (source: U.S. Department of Transportation, 2006)

3 Testing methods

3.1 Methods of dynamic adhesion testing

The classification of adhesion test methods has conventionally been into static and dynamic categories. Although static methods are helpful in detecting obvious deficiencies of cord rubber bonding, they are not sensitive to subtle changes. Moreover, the nature of the tests are not simulating the service condition of the tire. As a result, the data obtained in the laboratory is not an indication of the real performance properties of the product. Therefore, the dynamic tests are more meaningful as far as prediction of durability of tire is concerned. However, the dynamic test techniques are highly time consuming, costly and need extra capital investment (Chandra & Mukhopadhyay, 1995).

The dynamic adhesion test methods are classified into the three types, according to the type of deformation system that is used:

1. Tension test methods;
2. Compression test methods;
3. Flexing test methods.

3.1.1 Tension test methods

There are two types of tension test methods. The first is when the rubber is fixed and the cord/metal plate is tensioned directly (or reverse situation) creating a repeated shear of train to the cord-rubber boundary surface, and therefore a fatigue deterioration. This is the most frequently used method of evaluation of all the dynamic adhesion fatigue tests. This includes test methods such as the Buist method, the Vorachek method and the Wagner method.

The second one consists on a repeated tension peel method, this method is not as used as the one before due to the difficulties experienced in maintaining a constant peel surface and peel angle during a test and the difficulties that are experienced in connection with the accuracy of the peel force. However, the test machines are comparatively simple, and therefore there is a cost advantages. This includes test methods such as the Scott method and the Levit method (Mitsuhashi, 1981).

3.1.2 Compression test methods

There are two types of compressive adhesion fatigue tests. The first type consists on a falling weight repetitive impact type test method in which a fixed load, displacement and

energy can be carried out onto the rubber block. This includes test methods such as the A.P. Osborne method and the R.P. Campion method.

The second type involves the use of a flexometer in which a compressive deformation of fixed amplitude is applied under a fixed compressive load, simulating the situation in a running tire. This test may be inconvenient when many samples have to be evaluated. This includes test methods such as R.V. Uzina method and The P.P. Langevin method.

3.1.3 Flexing test methods

This method includes a rotation flexion and can be divided into two types. On the rotation type test methods, the sample is rotated in a large loop while applying a tension so that a flexing deformation is repeatedly applied to the sample. This includes test methods such as the J.R. Beaty method and the G.D. Mallory method.

The characteristic feature of the second flexing type methods is that a maximum tensile strain applied repeatedly at the point of flexure and the adhesion fatigue degradation due to the shear strain at the cord-rubber boundary surface is assessed. This includes test methods such as the G.A. Pittman method and the L.V. Cooper method (K.Mitsuhashi, 1981).

3.2 Adhesion Reinforcement test methods

3.2.1 Green Adhesion Test

Green Adhesion is a textile reinforcement test. This test method determines the Static Pull-Out Force of textile cord fabric from non-vulcanized calendered material. The Pull-Out Force is the maximum force or load expressed in Newtons, which a test specimen can support during a tensile test of loading to break (Bekaert Combustion Technology BV, 2016). This test evaluates and finds defects on the reinforcement cord and the rubber matrix before it goes under further process, allowing to prevent any further use of this material. Therefore, this test is a time and financial advance for the company.

The standard method used calendered textile fabric that must be protected against air humidity before testing. The sample must be prepared and tested immediately after been separated from the protective foil so that the test results are not negatively influenced from the moisture.

The test piece is fixed in the lower clamp and the cord fabric is pulled out in the upper clamp of the tensile test (fig.3.1). The test is performed on the Zwick Tensile Tester at room temperature, the cord is pulled vertically with a speed of 100 mm/min and five measurements

must be performed for each sample (Burghof, 2015). The sample preparation for this test is presented on the appendix A.1.

Figure 3. 1 - Illustration of the Green Adhesion Test

3.2.1.1 Parameter setting

The purpose of this test was to evaluate if the results from this test using different sample constructions would lead to results that could be related with the standard results. Therefore, two different sample constructions were performed instead of using the calendered fabric:

1. Using 5 dipped cords.
2. Using 5 calendered cords.

3.2.2 3-Cord Adhesion Test

The 3-Cord Adhesion Test is a steel reinforcement test that came across as a direct tension test and a peel test. This test determines the Pull-Out Force of steel cord, allowing to evaluate the adhesion between this and the rubber matrix and find the best conditions for a better bond. When compared to others dynamic test methods, this test is a time and financial advance for the company.

This test is able to determine the static and dynamic adhesion between the steel cord and the rubber matrix. The dynamic condition used in this test (fatigue deterioration) is performed over on the Frank Machine or the MTS Machine, depending on the chosen temperatures needed for the test. The fatigue consists on bending the sample for a fixed number of cycles, temperature and frequency.

After the sample curing, a waiting period of 3 hours is recommended before testing. The test piece is fixed in the upper clamp and 3 cords fabrics are pulled out by the lower clamp (figure 3.2). The test must be performed on the Zwick Tensile Tester at room temperature and the Force must be set zero to obtain comparable results between tests. The 3 cords are pulled vertically with pre-measurement travel of 20 mm till to guarantee that all tests have the same starting point and that the sample is conveniently clamped, then the test proceeds at 50 mm/min. Each sample is capable of performing five measurements. The sample preparation for this test is presented on the appendix A.2.

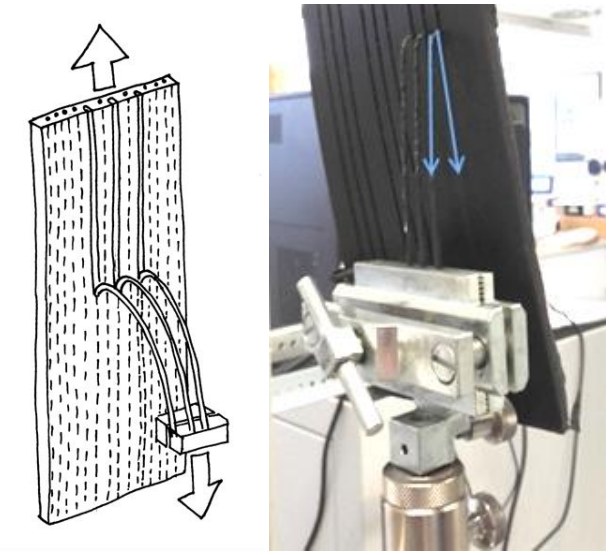

Figure 3. 2 - Illustration of the 3-Cord Adhesion Test (source: Thomas Felten, 2016)

3.2.2.1 Parameter setting

The purpose of this test was to determine the best standard conditions to perform the laboratory scale dynamic test using a less time-consuming procedure able to achieve results that match the tire real condition. Therefore, several tests were made until it has been defined the best set conditions. The conditions used for this evaluation are listed on figure 3.3, where it's defined the aging and the dynamic conditions.

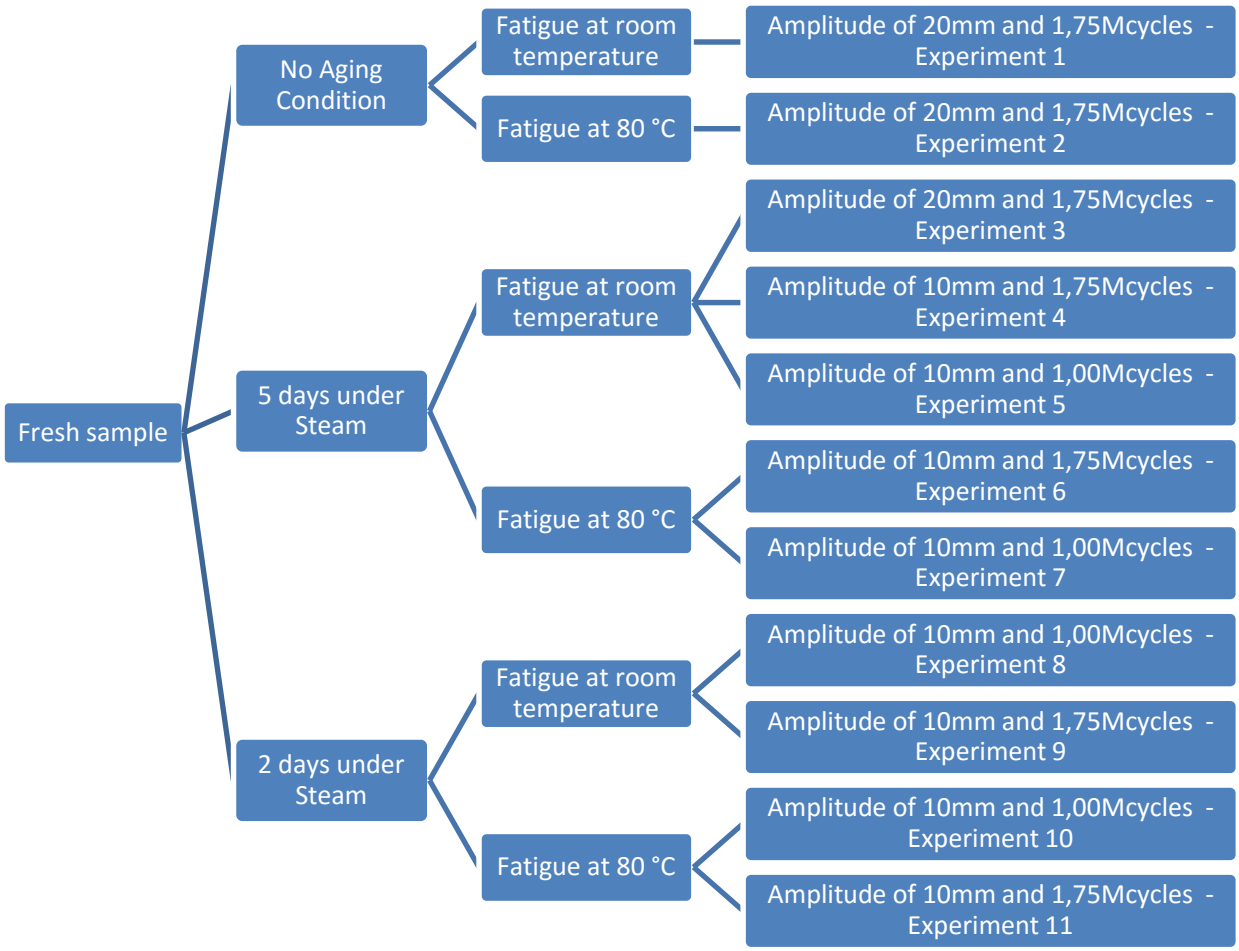

Figure 3. 3 - Conditions set for the 3-Cord Adhesion Test study

3.2.3 Dynamic T-Test

The Dynamic T-Test is a steel reinforcement test that is included in the direct tension test methods. This test determines the Pull-Out Force of steel cord from rubber matrix, allowing to evaluate the adhesion between this two and find the best conditions for a better bond. When compared with the other standard test performed in the company such as the Shear T-test, this allows the variation of the temperature due to the existence of a temperature chamber on the testing device (MTS Machine).

During the test the force level is increasing with higher number of steps (figure 3.4). Each step performs 200 cycles and with the increasing of next steps the level of the force reaches higher values and this is repeated until the cord detaches the rubber.

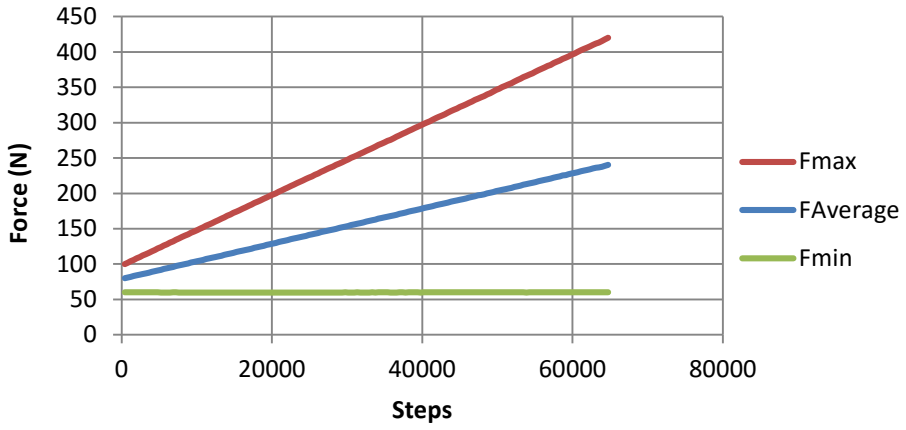

Figure 3. 4 - Graphic illustration of the increase of the force during the Dynamic T-Test (source: Thomas Felten, 2016)

This test has some advantages when compared to the 3-Cord Adhesion Test, it allows not only the evaluation of the force applied during the dynamic procedure and the determination of the Pull-Out Force, but also the number of cycles required for the sample to break, the complex dynamic stiffness and the phase lag.

The complex dynamic stiffness (K*) and the phase lag (δ) are two parameters that calculate the elastic and viscous effects (Frampton, 2009). The relation of force with the displacement (ΔF/Δx) obtains the complex dynamic stiffness (fig. 3.5).

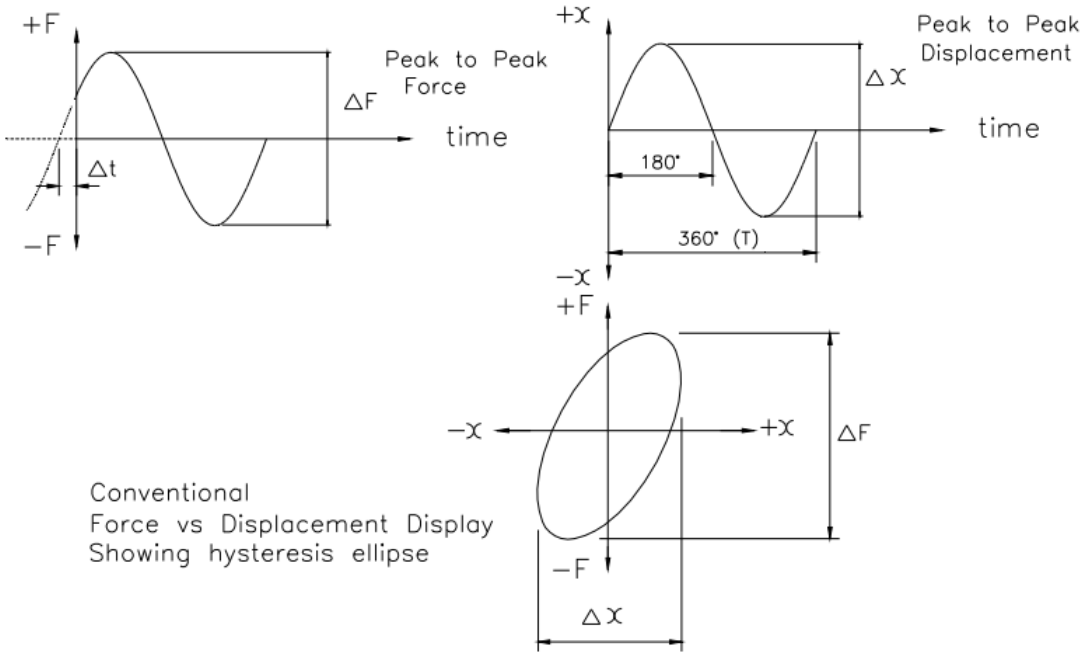

Figure 3. 5 - Measurement of Dynamic stiffness and phase lag (source: Frampton, 2009)

As observed on figure 3.6, the phase lag (δ) is simply the phase shift between the force and displacement waveforms (stress input and strain response) (Guelho, Reis, & Fontul, 2012). The relation between the time difference between the zero points of the two waveforms (Δt) and the period of the waveform (T) obtains the phase lag ($^{\Delta t}/_{T}.360°$). Usually is presented as tan(δ).

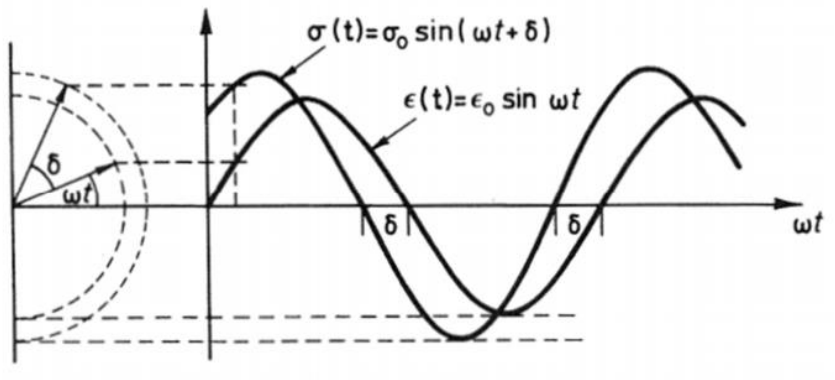

Figure 3. 6 - Phase lag between stress and strain (source: Guelho, Reis, & Fontul, 2012)

The Pull-Out Force is determined when the cord detaches the rubber and this corresponds to the maximum force that is obtained by the following equation:

$$\text{Pull} - \text{Out} - \text{Force} = \text{Static load applied} + \frac{\text{dynamic load applied}}{2} \quad (1)$$

The difference from the previous test is that in this one it's performed one cord at the time which means that each cord is pulled-out separately. Therefore, each sample must not contain more than 3 cords to avoid the effects caused by heating conditioning, that may affect the reproducibility of the results. The sample preparation is presented on the appendix A.3.

This test includes not only the MTS Machine but also a temperature chamber and the Hydraulic system. The cord is trapped on the upper clamp and the bottom part of the sample on the lower clamp (fig. 3.7).

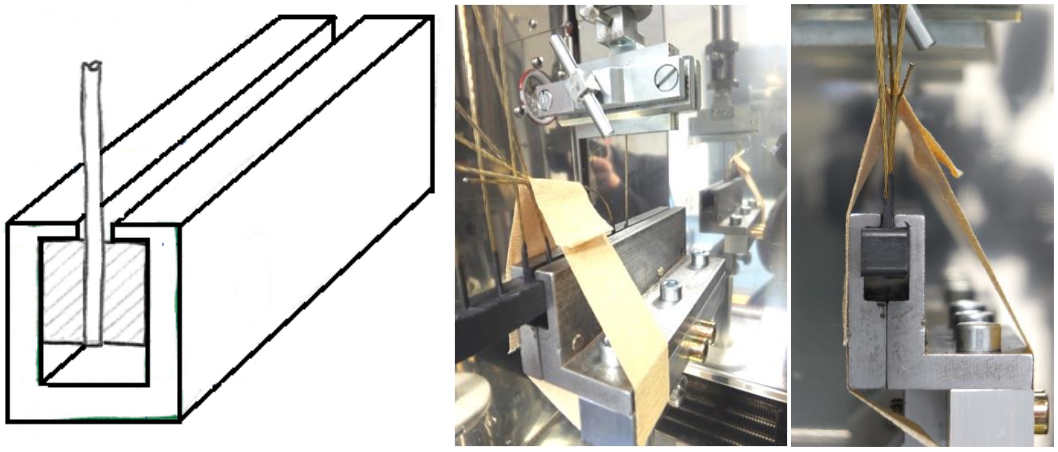

Figure 3. 7 - Illustration of the Dynamic T-Test (source: Thomas Felten, 2016)

The upper clamp moves according the amplitude of the step and is stopped when it's reached the Pull-Out Force (fig. 3.8). This test is performed at 80 °C, warming up at the same time the Hydraulic system in the Function Generator with a mean level of 20 mm, amplitude of 10 mm and a frequency of 1 Hz. Before running the test, the sample has to be pre-heated for 30 minutes, the displacement set to 0 mm and the axial force fixed to 5 N.

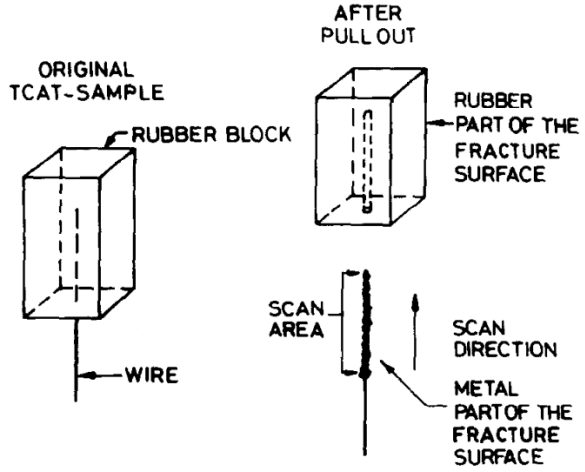

Figure 3. 8 - Sample before and after the test procedure (source: Arup K., 1996)

3.2.3.1 Parameter setting

The purpose of this test, like the 3-Cord Adhesion Test, was to determine the best standard conditions to perform the laboratory scale dynamic test. The conditions used for this evaluation are listed on figure 3.9, where it's defined the aging and the dynamic conditions.

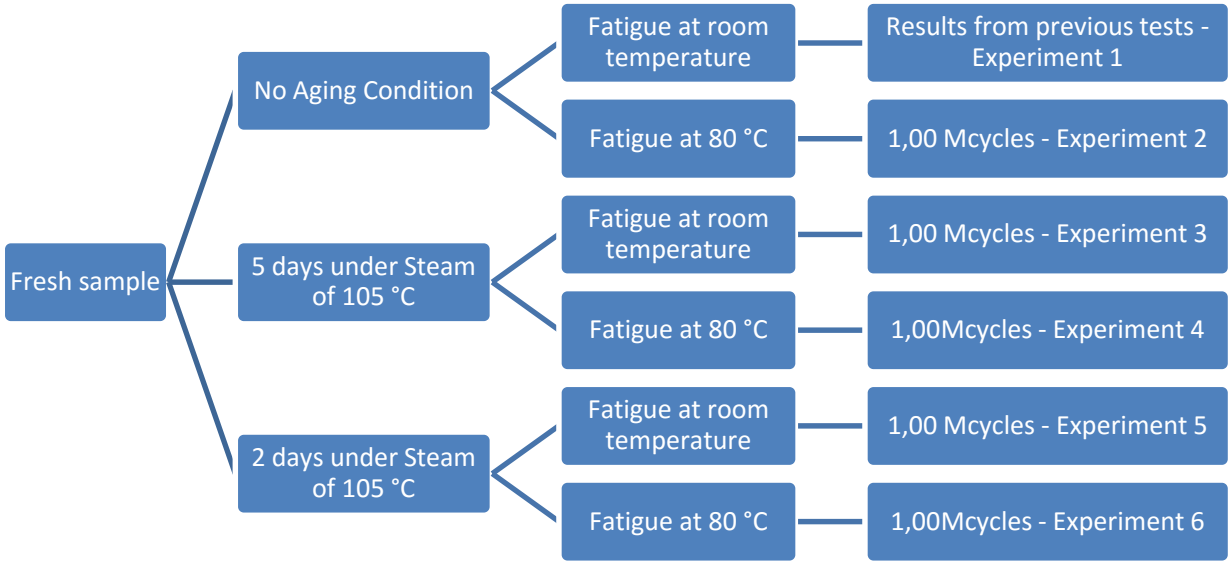

Figure 3. 9 - Conditions set for the Dynamic T-Test study

The results from the experiment 1 were obtained by previous tests performed under same conditions on the Reinforcement Testing Lab.

3.3 Aging and Fatigue conditioning

For these studies the aging conditioning performed was the steam exposition. The steam conditioning is performed at 105 ºC for 2 or 5 days. This sample is trapped in a container with water, carefully closed to prevent vapor leak and then inserted in the oven (fig.3.10). The effects caused by the steam exposition are described on the section 2.3.3.

Before this procedure the sample has to be covered with a anticorrosive special primer based on pure PVC-resin (REESA PVC-Primer 3G050). This is used as wash-primer at all steel-surfaces which needs additional protection against corrosion (REESA, 2016).

Figure 3. 10 - Container and Oven used for the Steam Conditioning

The fatigue is performed on the Frank Machine or on the MTS Machine and allows the sample to go under extreme conditions, like the real tire service conditions, in a short amount of time. The fatigue is achieved the creating a pre-load pressure on the sample (only executed on the dynamic t-test) and then a bending for 3-Cord adhesion test or an expansion for dynamic t-test (fig. 3.11) during a fixed number of cycles (fig. 3.12).

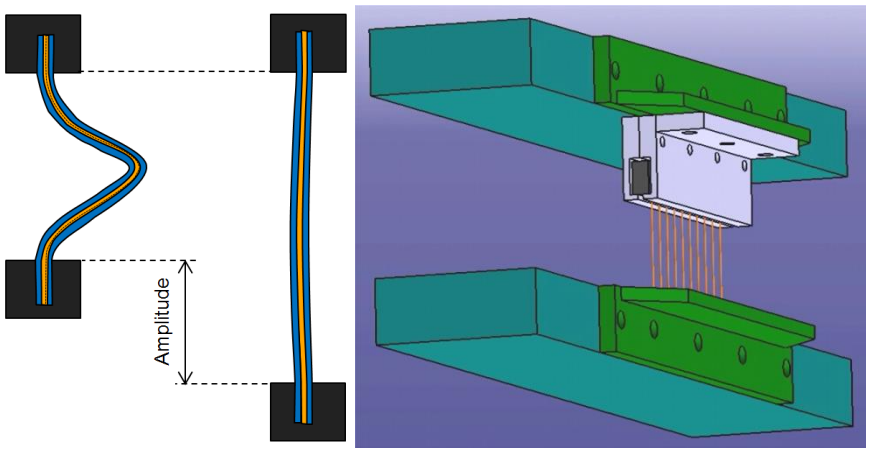

Figure 3. 11 - Illustration of fatigue on 3-Cord Adhesion (left) and Dynamic T-test samples (right) (source: Thomas Felten, 2016)

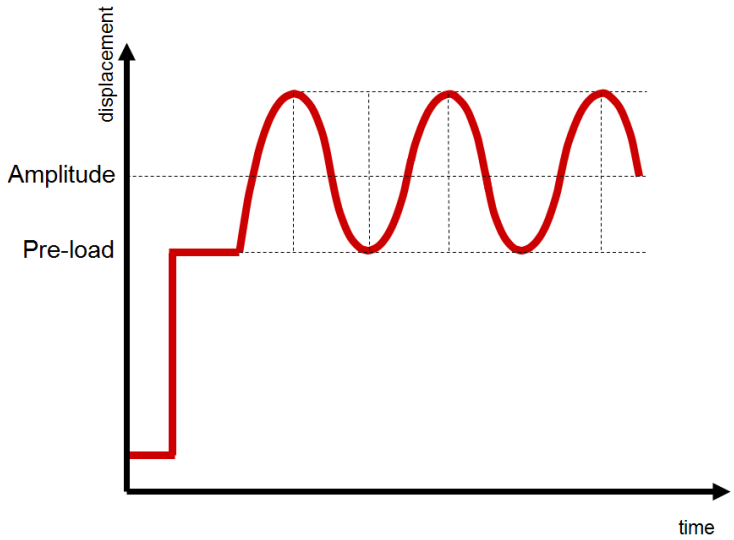

Figure 3. 12 - Displacement during the fatigue procedure (source: Thomas Felten, 2016)

The fatigue is performed by fixing the amplitude or the force. In these studies, the amplitude was the fixed parameter. In the fatigue performed over on the MTS Machine the force needed (maximum and minimum) was measured to evaluate its behavior during the test procedure (fig. 3.13).

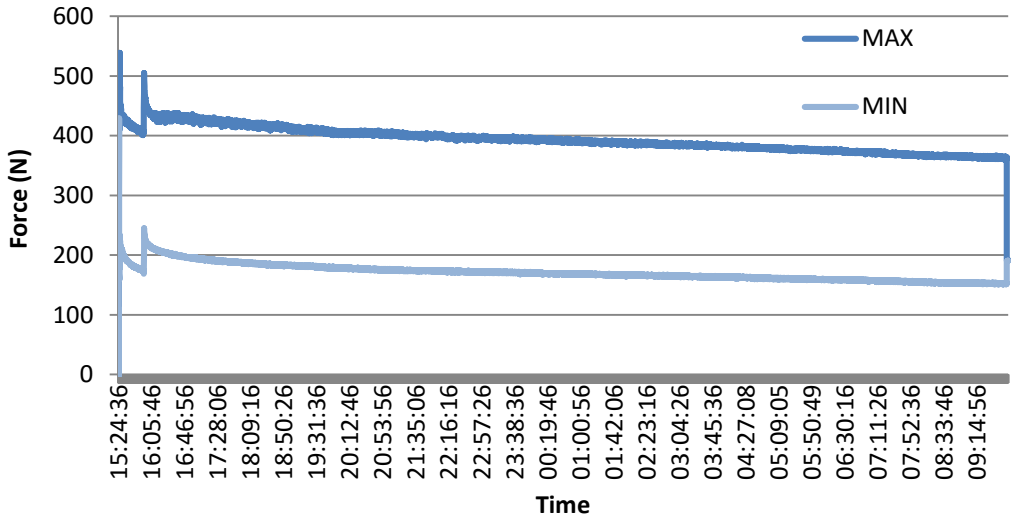

Figure 3. 13 - Evolution of the force during the fatigue procedure

The behavior of the force goes as expected, the value decreases during the fatigue test due to the fact that the sample's strength has decreased, confirming that the sample goes under conditions similar to the tire's service conditions.

The fatigue was performed with a fixed amplitude of 1.25 mm and a frequency of 8 Hz for the dynamic t-test samples and frequency of 5 Hz for the 3-cord adhesion test samples. The fatigue performed on the MTS machine operates at 80 °C and this is based on the work of Chandra, A. K. and Mukhopadhyay, R. in 1995 and Xinyan Shi and Mingqiang Ma in 2013.

3.4 Equipment

In order to perform the test analyses, the aging conditioning and the fatigue deterioration, for the steel and textile reinforcement test methods, different equipments were required. Below the main equipments used are enunciated:

3.4.1 Frank Machine

This equipment (fig. 3.14) was designed only for the purpose of fatigue deterioration (tension or compression) and can only work at room temperature. The fatigue is created by a tension deformation caused by the movement created by the bottom bar of the equipment. The fatigue is performed according the value for the different parameters: the amplitude that reach approximately 25 mm, the number of cycles that can reach 99 999 999 per test and the frequency that can reach up to 10 Hz however, this parameter is highly limited by the equipment for security reasons.

Figure 3. 14 - Frank Machine (source: Thomas Felten, 2016)

3.4.2 Zwick Tensile Tester

This Zwick Tensile Tester, also known as the AllroundLine, is the equipment used to perform the Green adhesion test and the 3-Cord adhesion test. This equipment can carry test speeds from 0.00005 to 3000 mm/min and it's independent of the test load, with test-area heights from 1030 mm to 2560 mm and test loads up to 250 kN (Zwick Roell, 2016).

The equipment requires different clamps depending on the test method to be perform, the Green adhesion test and the 3-Cord adhesion test, as shown on the figure 3.15.

Figure 3. 15 - Zwick Tensile Tester (left), clamps for the Green Adhesion (middle) and for the 3-Cord Test (right) (source: The Zwick Roell)

3.4.3 MTS machine

This MTS machine is the equipment used to perform the Dynamic t-test (fatigue and test procedures) and the 3-Cord Adhesion test fatigue procedure because, unlike the Frank machine,

this equipment is capable of operating under different temperatures and therefore, under real tire's conditions.

The MTS machine, also known as MTS 810 Material Testing System, delivers a broad array of testing capabilities for both low and high force static and dynamic testing. By selecting from a variety of force capacities, software and accessories, the system can easily be configured to meet your specific material or component testing needs. The system features: Force ranges from 25 kN to 500 kN; The ability to test materials ranging in strength from plastics to aluminum, composites and steel; The capability to perform a wide variety of test types from tensile to high cycle fatigue, fracture mechanics and durability of components (MTS System Corporation, 2006).

Like the Zwick Tensile Tester, this equipment requires different clamps depending on the test method to be perform, the 3-Cord adhesion test and the Dynamic t-test, as shown on the figure 3.16.

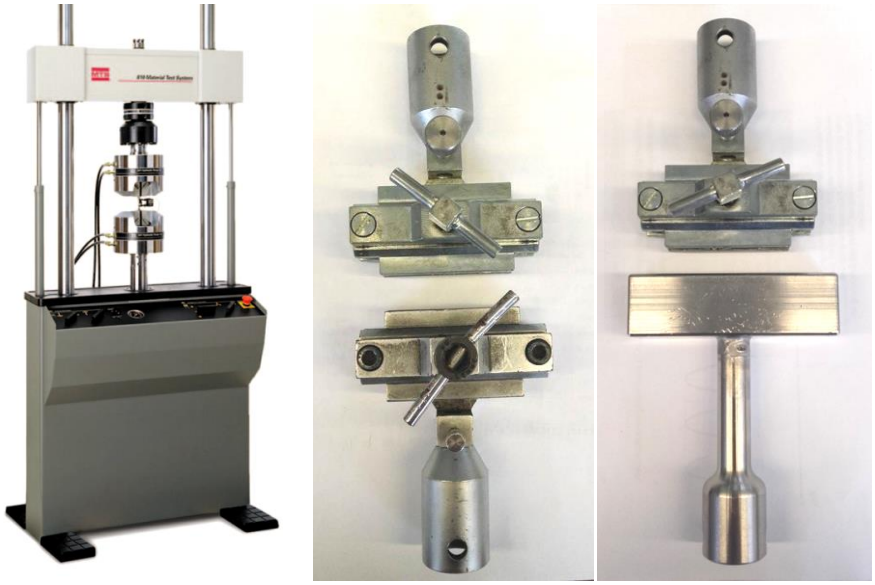

Figure 3. 16 - MTS Machine (left), clamps for the 3-Cord Test (middle) and for the Dynamic T-Test (left) (source: MTS Systems Corporation)

4 Results and discussion

4.1 Green Adhesion Test

The goal of this study was to evaluate if the use of different sample constructions would lead to results that could be associated with the standard results (using calendered fabric). The results from this test are presented on the appendix B.1. and its main results on the figure 4.1.

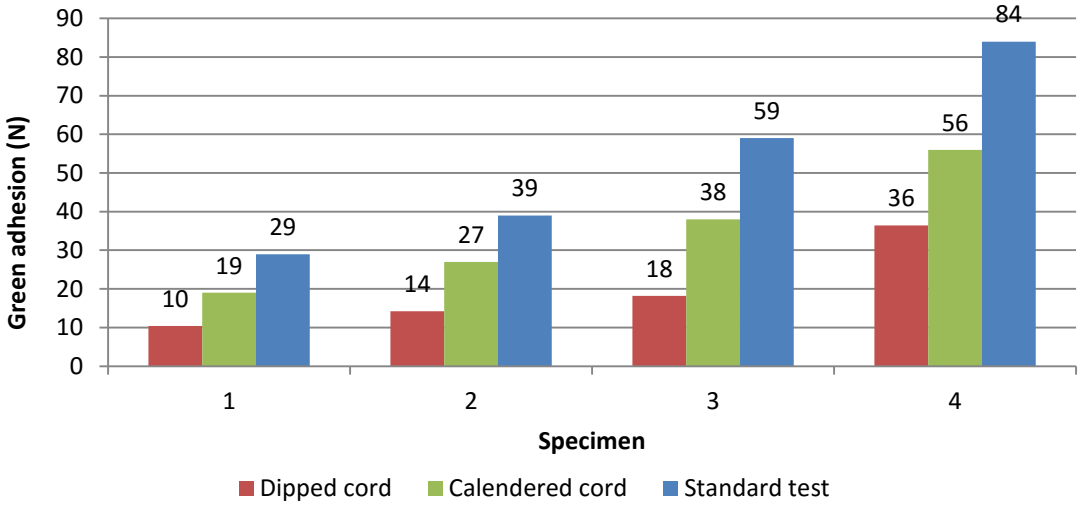

Figure 4. 1 - Test results from the new sample construction configuration and the standard results

The test results go according to the expected behavior: the value for the standard pul-out-force (using calendered fabric) was higher than using calendered cord due to the fact that the cords were not as loose, creating a stiffer sample and therefore a higher value of green adhesion. A bigger decrease happens when using dipped cord, because the absence of rubber involving the cord reduces the friction/adhesion between the rubber materials, allowing the cords to be more easily removed. The difference between the different specimens can be explained by properties shown on table 4.1.

Table 4. 1 - Properties of the test specimens

Specimen	1	2	3	4
Material	Nylon	PET	PET	Rayon
Cord thickness (mm)	0.30	0.63	0.75	0.82
EPDM[(1)]	120	121	105	104

[(1)] Number of cords incorporated per 10 cm of fabric

Increasing the cord thickness increases the surface area of the cord, allowing more rubber to cover the cord and as a result increasing the value of the green adhesion force.

PET does not contain as many polar functional groups as Rayon or Nylon, therefore a regular dipping procedure would not be enough for satisfactory adhesion. Due to the lack of polar and hydrogen bonding groups in its backbone structure, it is necessary to perform an activation of the textile substrate. In the case of nylon or rayon, they possess high surface polarities, as a result bonding mechanisms are very similar and take place between the RF resin and the cord surface (Louis, Noordermeer, Dierkes, & Blume, 2014).

However, this behavior is not being shown on the figure 4.1, due to different values of thickness between cords. For further evaluation, the test results of green adhesion were related to the cord thickness as shown on figure 4.2.

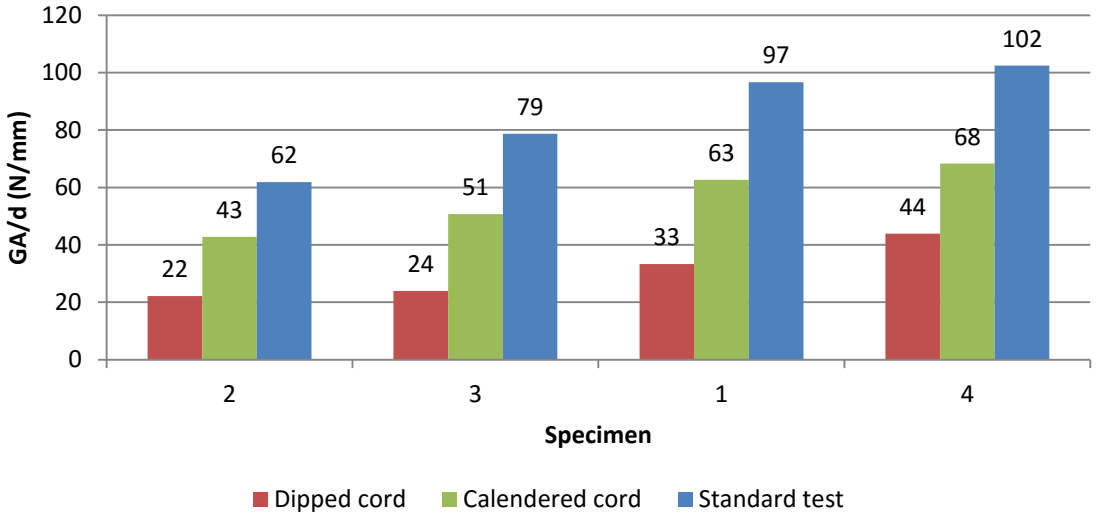

Figure 4. 2 - Relation of the green adhesion with the cord thickness for the different materials and sample constructions

Now the results are according to the expected behavior explained previously and the difference between the rayon and nylon results (rayon has higher results) is because rayon has a larger concentration of oxygen in its molecular chain. Furthermore, it was possible to conclude that, for the samples with the same material (PET), the decrease of EPDM shown higher values of green adhesion.

Increasing of the EPDM means there's a smaller distance between cords, allowing less rubber to penetrate the cord and reducing the value of green adhesion. However, this factor cannot be considered to evaluate the difference specimens because of the high deviation of cord thickness.

For further study, it was measured the decrease of the pull-out-force for the different specimens as shown on figure 4.3.

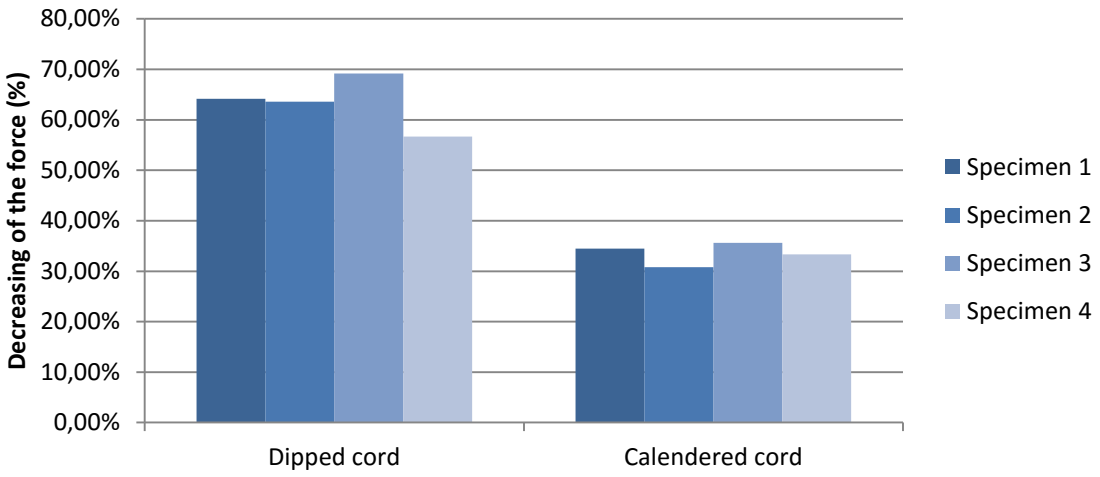

Figure 4. 3 - Decreasing of the green adhesion for the test specimens

The results allowed to conclude that, for each sample construction configuration, there was a homogeneous reduction of the pull-out-force. The test using dipped cord got a reduction of 63.4 ± 5.1 % of the standard value and the use of calendered cord of 33.5 ± 2.3 %. The value of the deviation was higher when used a dipped cord configuration due to the fact that the test values were too low and the equipment didn't have the capacity and precision to measure these.

To conclude, these positive results were an indicator that this test can be used for further studies of the adhesion capabilities of textile reinforcements in rubber using non-vulcanized material.

4.2 3-Cord Adhesion Test

Part of the study of the 3-Cord Adhesion test was to identify the best set conditions in order to obtain the most accurate results using less time consuming parameters and eliminating any sources of error. For this, three aspects regarding this method were studied before performing any study of the adhesion between steel cord and rubber: The influence of the sample's thickness in the results; the best configuration to set zero to the equipment; the reproducibility of the results from different samples.

The previous measurements performed in the company shown an unstable pull-out-force for all values of the strain creating the necessity of evaluating the influence of the sample's thickness on the test results. Figure 4.4 shows the difference between an undesired and a desired result, in which the standard force tends to remain the same during the test.

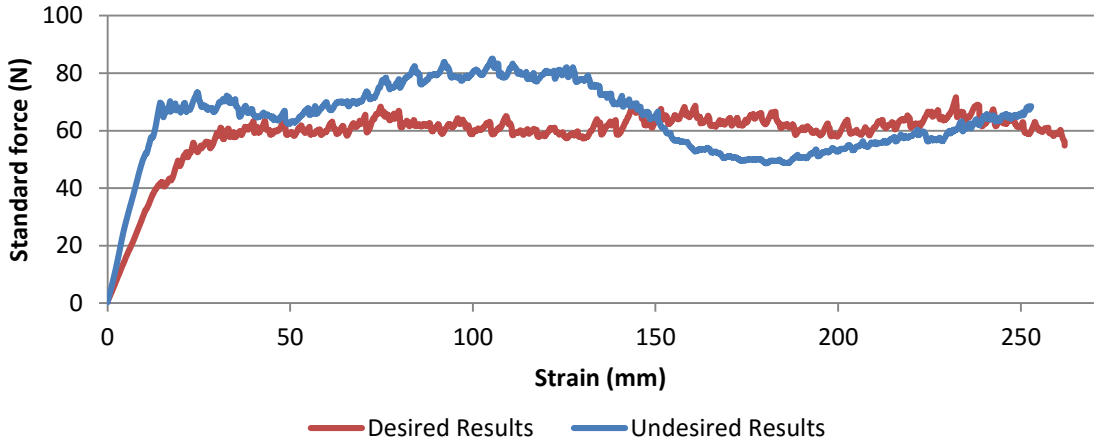

Figure 4. 4 - Graphic representation of a desired and an undesired test result

The samples are not completely homogeneous and present small deviation of the thickness. This study was performed on a sample with 3 cord sets and the results are described in the appendix B.2.1. The thickness of the sample was measured in 16 points (8 on the left side of the sample and 8 on the right side).

After the test had been performed, the values of the force were modified by nominating one point as a reference and creating a ratio to the other values, depending on the thickness of the sample at the measured point. The results regarding the non-modified values and the modified values are presented in the appendix B.2.1 and the comparison between these are presented on table 4.2.

Table 4. 2 -Test results of the highest and lowest pull-out force

	Non modified results (N)		Modified results (N)		Reduction (%)	
	Highest value	Lowest value	Highest value	Lowest value	Highest value	Lowest value
Cord set 1	148.061	78.952	147.286	78.516	0.524	-0.552
Cord set 2	165.171	105.450	164.535	105.325	0.385	-0.119
Cord set 3	161.480	111.280	160.188	113.490	0.800	1.986
				Average	0.504	

It was possible to conclude that the highest value all the Cord sets suffer a drop, however, on the lowest values only the Cord set 3 got a higher force. The average reduction was 0.504%, concluding that the thickness of the sample is not a critical factor for 3-Cord adhesion performance.

The start of the test procedure was also an important aspect for the test to obtain more homogeneous results. For this evaluation 3 samples, prepared under the same conditions, were tested under different configurations (fig. 4.5):

1. The zero is set when the sample is trapped onto the upper clamp (a);
2. The zero is set when the sample is also trapped onto the lower clamp (b);
3. The zero is set when the sample is in the position to start the test (c).

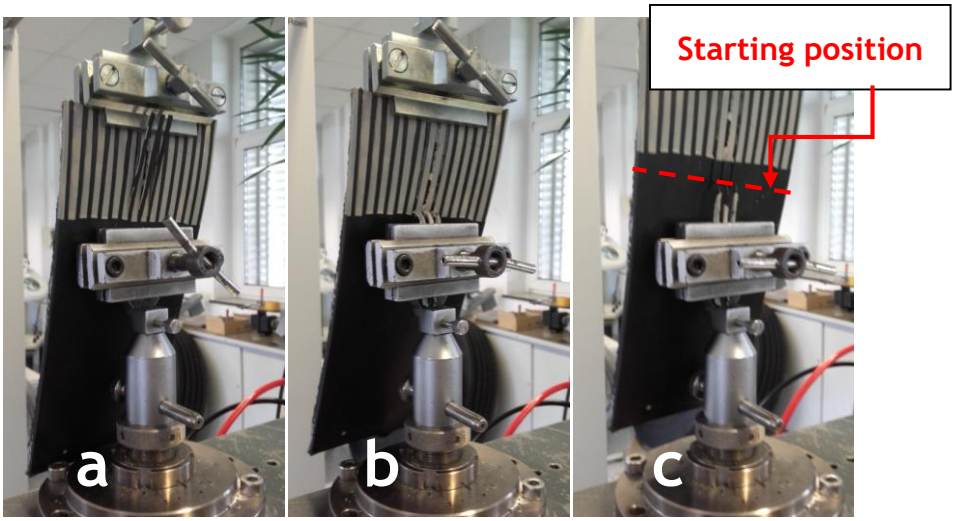

Figure 4. 5 - Illustration of the different set conditions to perform the test

The results for each sample are illustrated in the appendix B.2.2 and its main results on the table 4.3, where it's shown the initial deviation, the average deviation and the minimum and maximum deviation value. The deviation value is obtained by comparing the results from the value of the different cord sets in the point of strain.

When comparing the results, it was possible to exclude the third configuration because of the several negative values of pull-out-force.

Table 4. 3 - Test result deviations for the first and second test

	Deviation			
Test	Initial	Overall	min	max
First	12.36 %	11.35 %	0.14 %	29.07 %
Second	11.71 %	10.09 %	0.17 %	25.27 %

It was possible to conclude that, despite the fact that the first test has a lower value of minimal deviation than the second test, the second test shows better results in all the other parameters. Therefore, it was concluded that the second test presented the best conditions to

provide better results. To confirm this assumption, it was also studied the accumulation of the deviation for each sample (figure 4.6).

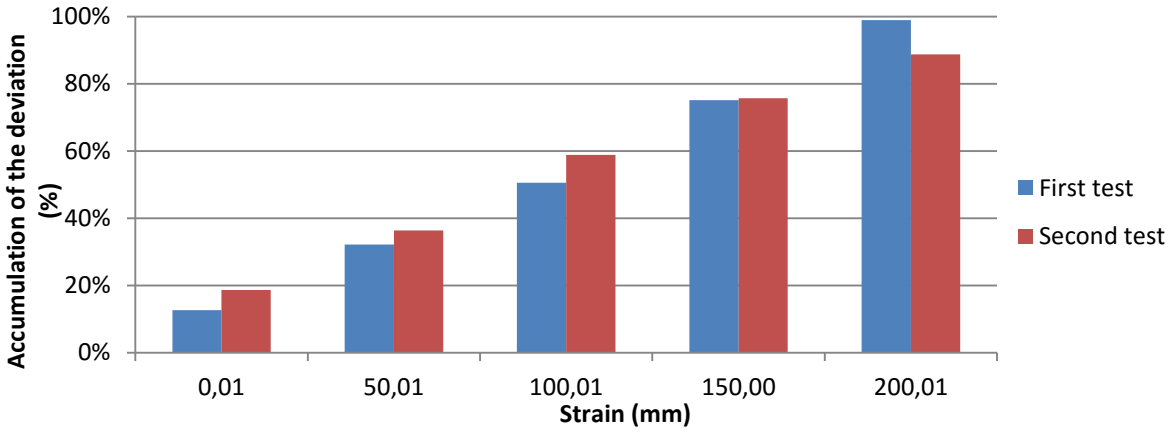

Figure 4. 6 - Evaluation of the deviation for the different test throughout the test procedure

The previous graph confirmed what was concluded previously, despite the fact that in the first values of strain the second test presents higher values of deviation, in the overall test the second test presented a lower value of accumulation of deviation (10.68 % lower than the first test).

To evaluate the reproducibility of the results, 3 samples with 4 cord sets each were prepared separately under the same conditions, tested and then compared to each other. The results are shown on figure 4.7. The third sample only included 3 cord sets because of an incorrect measurement done on one of the cord sets.

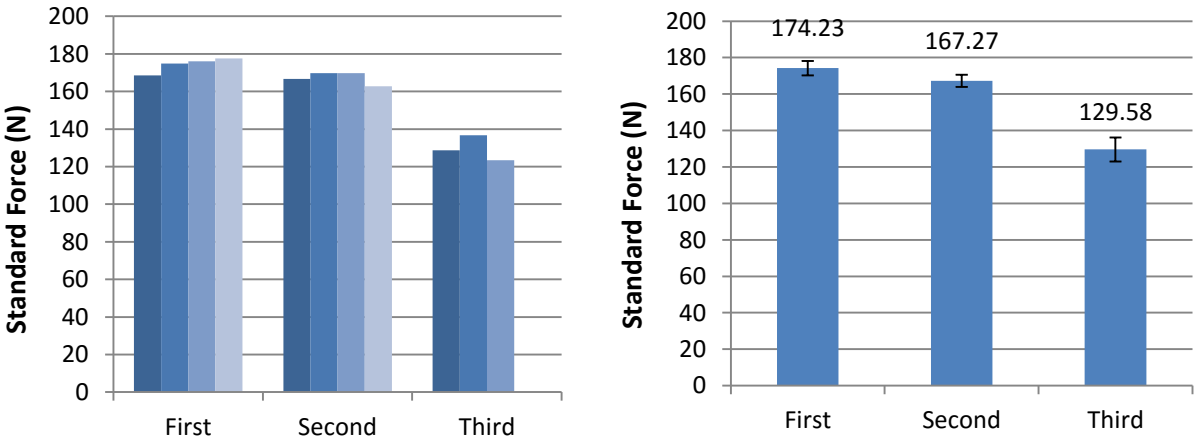

Figure 4. 7 -Test results for the different samples (left) and its average values (right)

It was possible to conclude that the 3 samples had different values of pull-out-force: 174.23 N, 167.27 N and 129.58 N, having a standard deviation of 24.03 N and therefore cannot be related for further tests. However, it was shown that for each sample the results were

homogeneous and therefore it was determined how the same sample could be performed under different conditions. The figure 4.8 represents the configuration established for the sample to be under an aging condition as well as a fatigue procedure without losing the symmetry needed to do it.

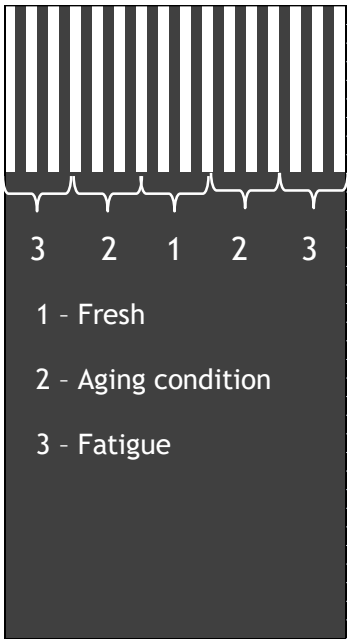

Figure 4. 8 - Set conditions of the sample to perform the 3-Cord adhesion test

After these tests it was also possible to point the reason for the undesired behavior of the standard force's curve along the strain of the sample, pointed on figure 4.4. This behavior is connected with the contact between the lower clamp and the sample, this created a friction during the test procedure and increased the value of the standard pull-out-force (fig. 4.9). Right when this contact is over the value tends to decrease.

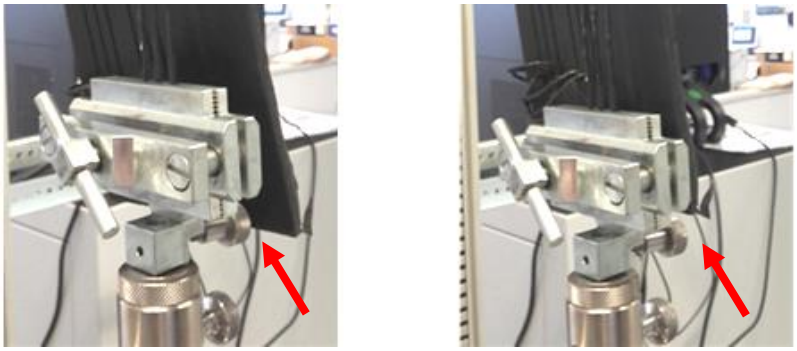

Figure 4. 9 - Illustration of the friction occurrence during the test procedure

After all these parameters have been set, the next step was the procedure explained on chapter 3.2.2, to determine the best standard conditions to perform the 3-Cord adhesion test,

optimizing the time-consumption and achieving results that match the tire real condition. The results from this study are presented on the appendix B.2.4.

When the fatigue was performed on the Frank machine (experiments: 1, 3, 4, 5, 8 and 9) no results were conclusive or beneficial for the test. These experiments (fig. 4.10 to 4.13) show that, regarding the time exposition of the sample to steam condition, there was no decreasing of the pull-out force (the pull-out force before and after the fatigue condition tended to remain the same) (fig. 4.10 and 4.11)

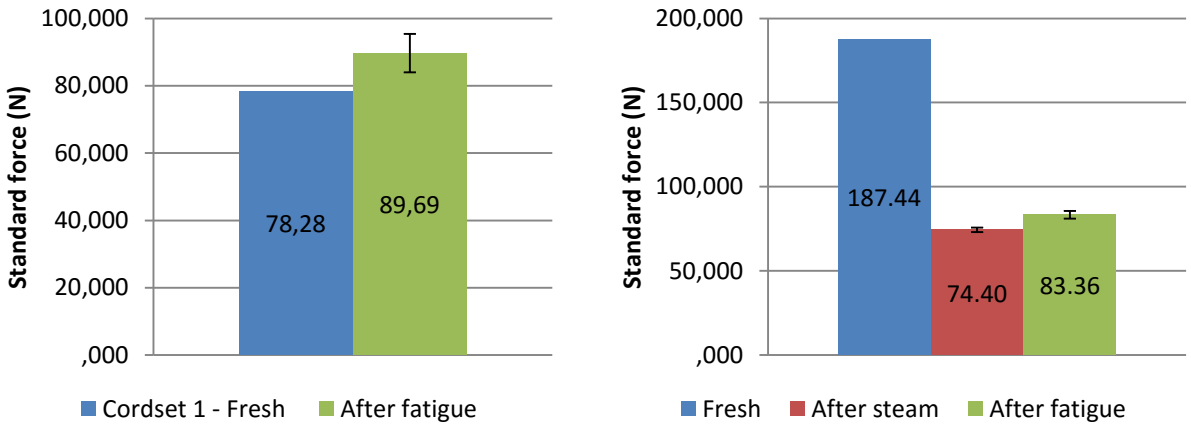

Figure 4. 10 - Test results from experiment 1 (left) and experiment 5 (right)

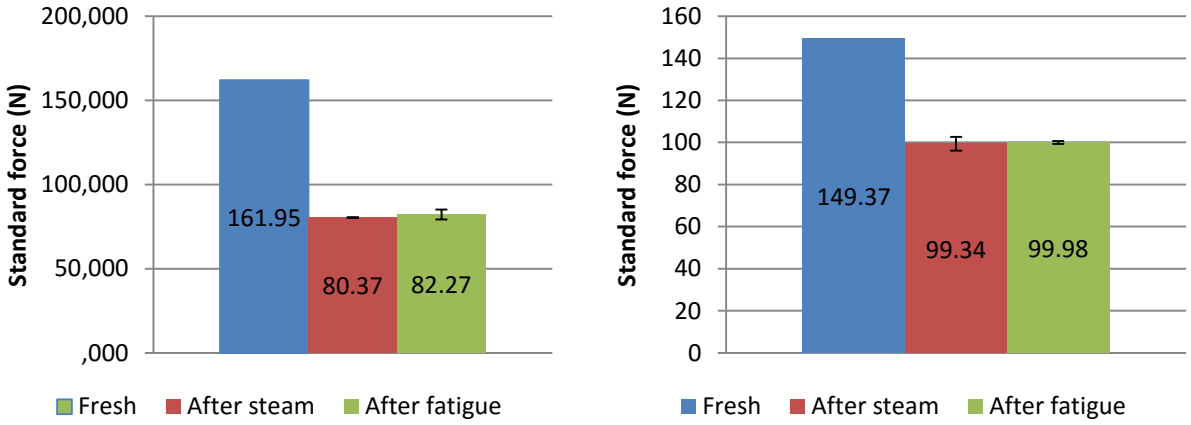

Figure 4. 11 - Test results from experiment 8 (left) and experiment 9 (right)

The previous results showed no reduction of the pull-out-force. Some results actually showed an increase of the pull-out-force, which goes against the predicted behavior. During the fatigue, the sample goes under extreme conditions, similar to the tire's service conditions, to allow the sample's strength to decrease, which means, to lower the adhesion between the steel cord and the rubber matrix.

For the experiments 3 and 4 it was not possible to measure the pull-out force due to the fact that the samples reached their limits and broke during the fatigue procedure or during the test procedure, as shown on figures 4.12 and 4.13.

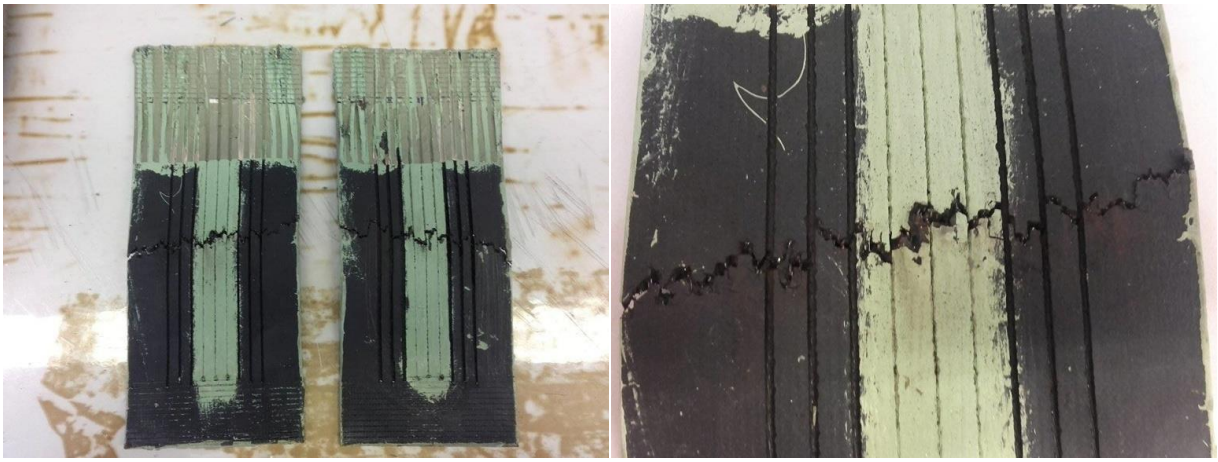

Figure 4. 12 - Samples from experiment 3 after fatigue

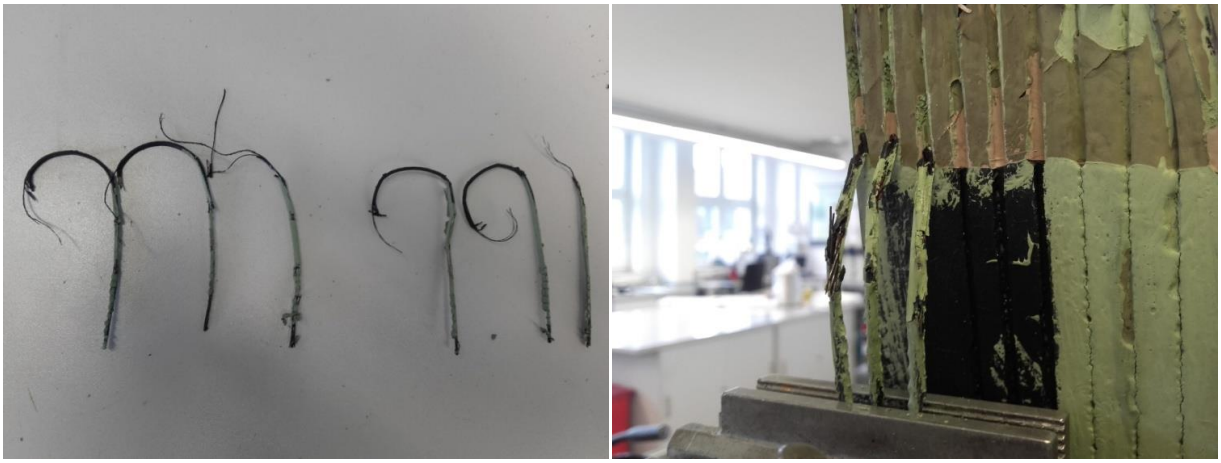

Figure 4. 13 - Samples from experiment 4 after fatigue

In these tests the fatigue conditions were too extreme for the sample's capacity, causing the sample to break.

The Frank machine is not a proper equipment choice to perform the fatigue due to the fact that it is limited to perform at room temperature. The results measured at room temperature cannot be considered as the composite’s performance in the utilization condition. Although heat buildup occurs in the test samples during the fatigue test procedure, this is not enough to illustrate the decreasing effect of the pull-out-force. Therefore, this configuration could not predict the cord/rubber system durability. In some studies, it is required to install a

heat chamber on the fatigue test, to produce more reliable results (Jamshidi, Afshar, & Shamayeli, 2006).

The first performed test on the MTS machine was the experiment 2, in which it was not used any aging condition and the results are shown on figure 4.14.

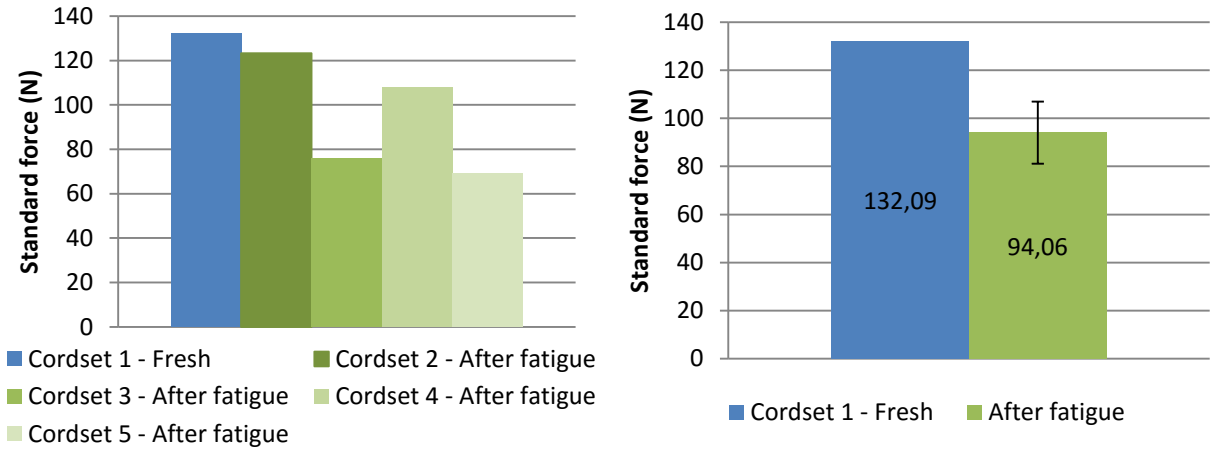

Figure 4. 14 - Test results from experiment 2 (left) and its average results (right)

Unlike what occurred on the Frank machine, on this test the value of the pull-out-force decreased because the equipment allows to use a higher temperature. However, as shown on the figure 4.14, the test didn't achieve a homogeneous reduction, this being an average decrease of the force of 28.80 ± 19.57 %. The value of the standard deviation is too high concluding that the sample has mandatorily to go through an aging procedure to obtain a steadier value.

When the fatigue was performed after a steam conditioning of 2 days (experiments 10 and 11) there was a consistent decreasing of pull-out-force with a small deviation. The reductions of the force were 57.60 ± 2.03 % and 31.54 ± 4.39 %, respectively. The results of these tests are shown on figure 4.15.

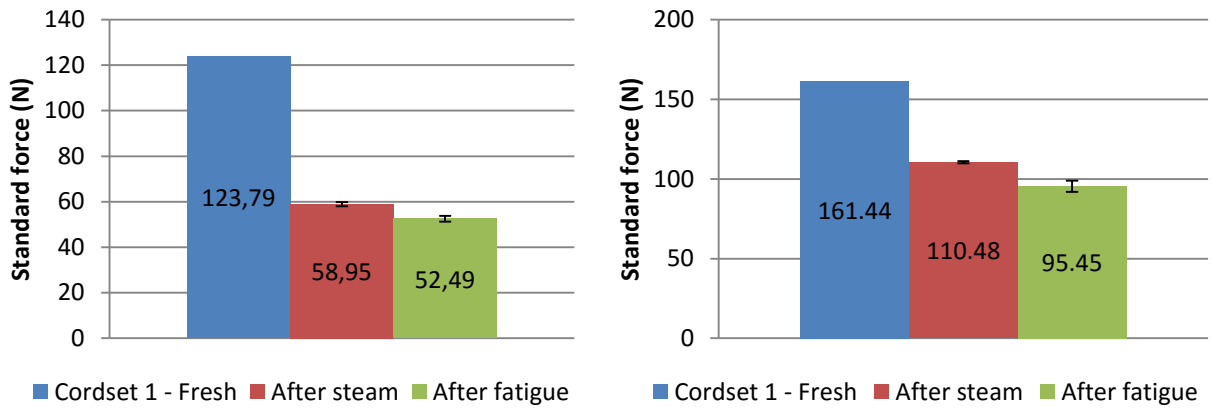

Figure 4. 15 - Test results from experiment 10 and experiment 11

Despite this, the reduction of the pull-out force between the steam aging and the fatigue were 5.22 % and 9.32 %, respectively. The decrease between these two steps is not enough to set these as the standard conditions.

When the fatigue was performed after a steam conditioning of 5 days (experiments 6 and 7) there was a consistent decrease of pull-out-force with a small deviation as well as a clear decrease of the force between the aging and the fatigue conditioning, as shown on the figure 4.16.

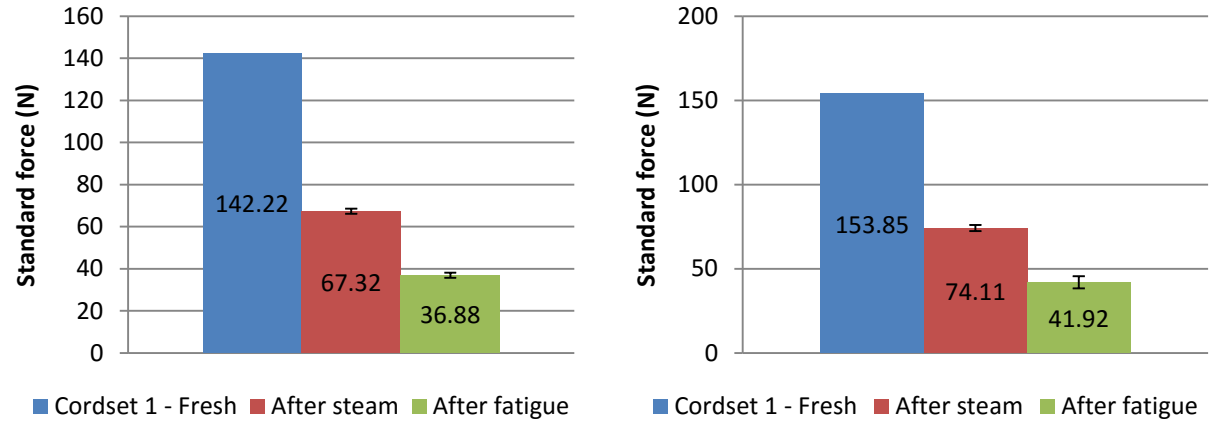

Figure 4. 16 - Test results from experiment 6 and experiment 7

The reductions of the pull-out-force were 74.06 ± 0.89 % and 72.75 ± 4.62 % and the differences between the difference between the pull-out force after steam and fatigue were 21.40 % and 20.92 %, respectively. Both test are good set conditions to perform the test however, the conditions used on the experiment 7 (Aging condition: 5 days under Steam;

Fatigue: 80 °C; Amplitude 10 mm; 1.00 million cycles) were chosen as the ideal conditions because it consumes less time and achieves similar results as the experiment 6.

To conclude, the best set conditions for the 3-Cord adhesion test are an aging condition of 5 days under steam and a fatigue deterioration at 80 °C with an amplitude 10 mm and 1.00 million cycles.

4.3 Dynamic T-Test

The main goal of the Dynamic T-Test was, as in the previous method, to determine the best standard conditions to achieve accurate results that match the tire real condition using less time-consuming parameters.

The best set conditions can be spotted by analyzing the decrease of the pull-out-force and the number of cycles and the evolution of the complex dynamic stiffness and the phase lag during the test procedure. The results from this study are presented on the appendix B.3.

Both the phase lag and the complex dynamic stiffness were not helpful variables to evaluate the different set conditions. As shown on appendix B.3, the phase lag values had similar values regarding the condition that they were submitted and high levels of deviations. The complex dynamic stiffness showed no consistent behavior throughout the aging and fatigue conditioning and in some cases high levels of deviation. Due to this fact the parameters that allowed the determination of the best standard were the pull-out-force and the number of cycles.

Like what succeeded on the 3-Cord adhesion test, when the fatigue was performed on the Frank machine (experiments: 1, 3, and 5), the results showed no reduction of the pull-out-force or the number of cycles (fig. 4.17 to fig. 4.19).

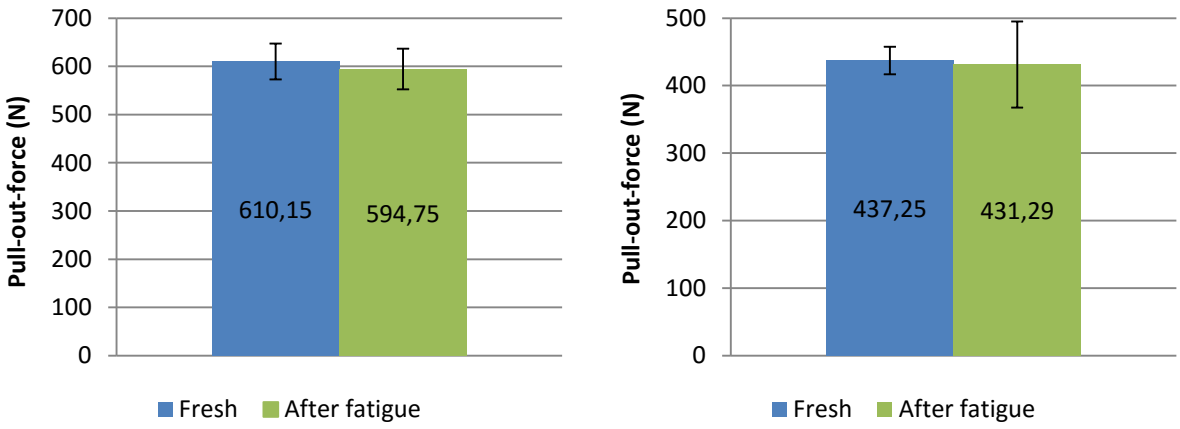

Figure 4. 17 - Test results from two different samples for experiment 1

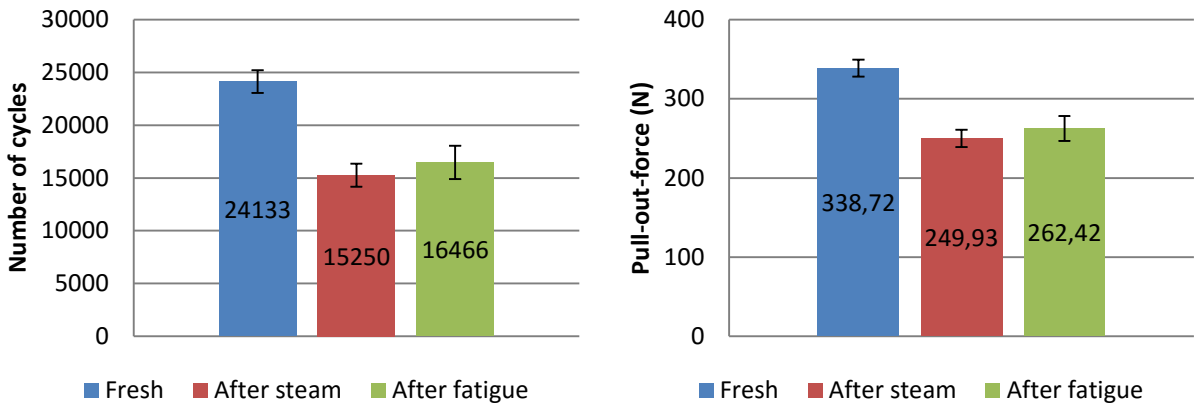

Figure 4. 18 - Evolution of the number of cycles (left) and pull-out-force (right) on experiment 3

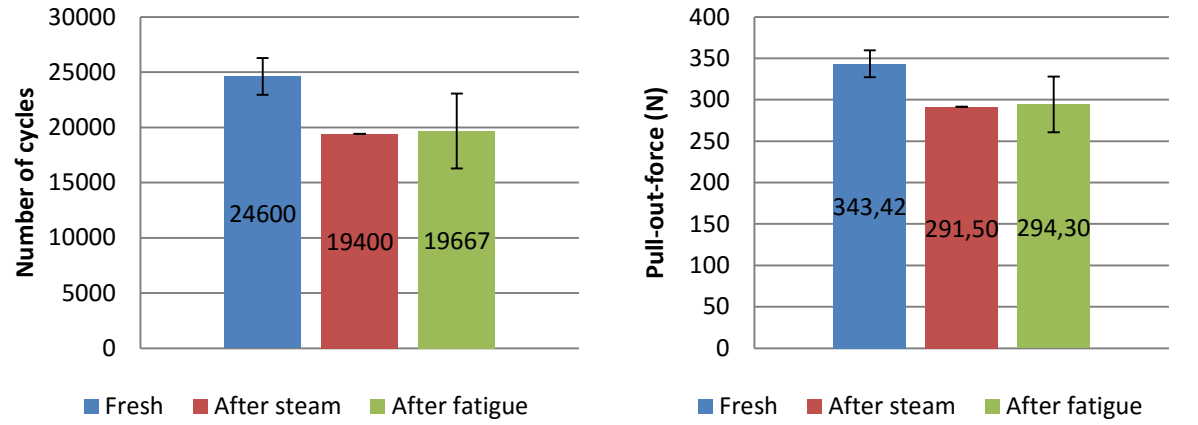

Figure 4. 19 - Evolution of the number of cycles (left) and pull-out-force (right) on experiment 5

Beside the high deviation of the different parameters, it's possible to notice that there was no decrease of the pull-out-force. Like it was concluded previously, the fatigue didn't show any reduction of the pull-out-force due to the fact that it was performed at room temperature. Therefore, for both steel test methods, this configuration could not predict the cord/rubber system durability, concluding the fatigue must be performed at a higher temperature to achieve the expected results (Jamshidi, Afshar, & Shamayeli, 2006).

When the fatigue was performed at a higher temperature (experiment 2, 4 and 6) there was a clear reduction of the number of cycles and the pull-out-force, regardless of the aging conditioning (fig. 4.20 to 4.22).

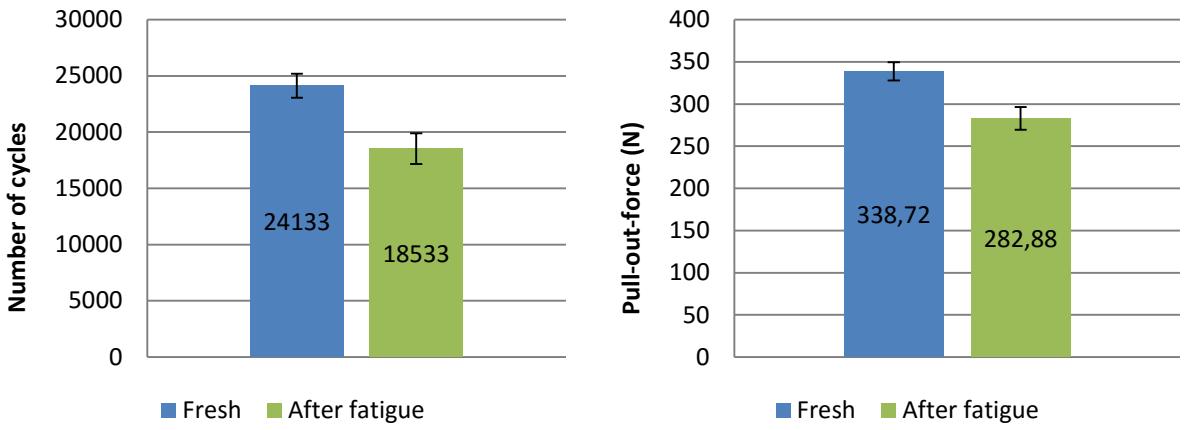

Figure 4. 20 - Evolution of the number of cycles (left) and pull-out-force (right) on experiment 2

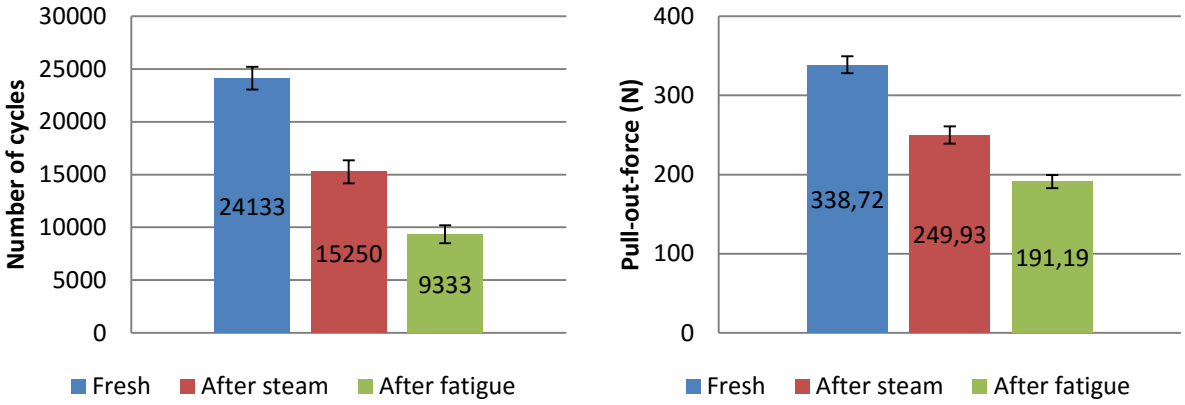

Figure 4. 21 - Evolution of the number of cycles (left) and pull-out-force (right) on experiment 4

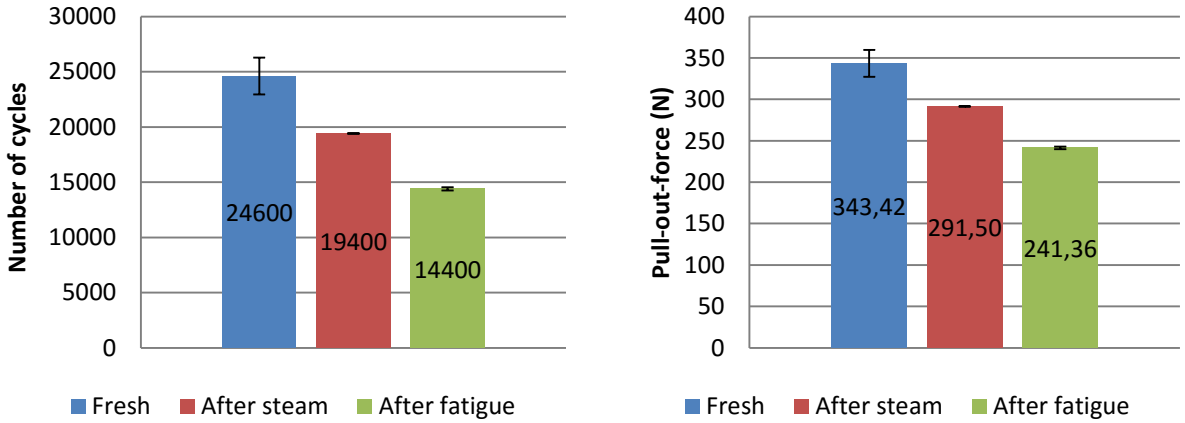

Figure 4. 22 - Evolution of the number of cycles (left) and pull-out-force (right) on experiment 6

The reductions of the pull-out-force were 16.49 ± 7.93 %, 43.56 ± 4.98 % and 29.72 ± 0.98 % for the experiment 2, 4 and 6. The experiment without steam conditioning (experiment 2) was excluded because of its low value of reduction and high value of deviation. The sample needs a steam condition to allow a bigger and homogeneous reduction of the force.

Regarding the experiments 4 and 6, the force reduction between the aging and the fatigue conditioning was 17.34 % and 14.60 %, respectively. This allowed concluding that the extend exposition of steam didn't have an impact on the reduction happening on the fatigue step.

Due to the fact that the experiment 6 was only able to achieve a reduction of 29.72 % this was excluded as the best set conditions for the test. Therefore, the conditions used on experiment 4 (Aging condition: 5 days under Steam; Fatigue: 80 °C; 1.00 million cycles) were chosen as the best set conditions to perform the test. However, when compared to the 3-Cord adhesion test which achieves a reduction of approximately 70 %, this is only able to obtain roughly 45 % which may not be enough for the new compound recipes and therefore an additional increase of the number of cycles on the test should be included.

The next step was to test both steel methods using these test set conditions on the new compound recipes however, due to the lack of time of the internship this was not possible to execute and will have to be taken by account for a further study of the dynamic tests.

4.4 3-Cord Adhesion Test Vs Dynamic T-Test

When compared the 2 different steel reinforcement test methods, there are clear differences as well as similarities between these two that could affect the company's choice on which to choose depending on the goals of the study. The main differences and similarities between the test methods are shown on the table 4.4. The table consists on a personal evaluation based on the experience of working with both methods during the development of the best standard conditions for both.

Table 4. 4 - Differences and similarities between the 3-Cord Adhesion Test and Dynamic T-Test

	Dynamic T-Test	**3-Cord Adhesion Test**
Number of samples per test	3 (with 3 cordsets each)	1 (with 5 cordsets)
Procedure time (testing)	2.5 hours	15 minutes
Procedure time (total)	6 days	9 days
Parameters tested	Pull-out-force; Number of cycles; Complex dynamic stiffness; Phase lag	More accurate pull-out-force

Testing procedure	Complex	Simple
Fatigue procedure	Requires mechanical precision and longer setup time	Simple
Required equipment	MTS machine	MTS machine and Zwich and Tensile Tester
Predicted force reduction	~ 45 %	~ 70 %
Required Raw material	Uses small amounts	

In conclusion, if the goal is to achieve fast results using a more cost-effective test the chosen procedure should be the Dynamic t-test. This is based on the fact that the Dynamic t-test requires the use of less equipment and is a less time-consuming method because the samples can be set to different conditions separately and the fatigue procedure has a higher value of frequency. The biggest disadvantages of this method are that it involves a complex procedure of fatigue and testing and the pull-out-force is measured with the average of only 3 cords.

If the goal of the study is to obtain a more precise and accurate value of the pull-out-force, the chosen procedure should be the 3-Cord adhesion test. This method is able to achieve a high percentage of force reduction and evaluate the pull-out-force throughout the sample and generate an average value accounting more than 13 000 measurements. However, this method takes more time and requires the use of two equipments.

5 Conclusions

The focus of this thesis was to determine the best standard conditions to perform a laboratory-scale dynamic test on samples containing the new desired composition (new compounds with reduced incorporation of resorcinol) able to achieve results that match the tire real condition, using a less time consuming test such as the Dynamic t-test and the 3-Cord test.

Another project later included in the thesis regards a textile reinforcement test method, named Green Adhesion test. The goal of this study was to evaluate if the use of different sample constructions would lead to results that could be compared with the standard results provided from the Lousado plant in Portugal.

For both steel reinforcement test methods the best standard conditions were obtained, these being an aging condition of 5 days under Steam and fatigue at 80 °C, with an amplitude of 10 mm and 1.00 million cycles for the 3-Cord adhesion test and an aging condition of 5 days under Steam and fatigue at 80 °C during 1.00 million cycles for the Dynamic t-test.

For both methods, the fatigue showed a clear decrease of the pull-out-force: 72.75 ± 4.62 % and 43.56 ± 4.98 % when performed on the MTS machine. The results measured at room temperature cannot be considered as the composite's performance in the utilization condition. The decrease of the pull-out-force only occurred when the test was performed at higher temperatures than the room conditions, even though self-heating of the sample occurs during the fatigue procedure, this wasn't enough to have an effect on the results.

The 3-Cord adhesion test was able to achieve positive results in approximately 9 days and the dynamic t-test in 6 days. Concluding that both showed a time and financial advantage for the company when compared with the current standard test used (Drum-test).

The results of the Green adhesion test revealed that, for each sample construction configuration, there was a homogeneous reduction of the green adhesion force. The test using dipped cord got a reduction of 63.4 ± 5.1 % and the use of calendered cord of 33.5 ± 2.3 %. This allowed to conclude that these sample constructions can be used for further studies of the adhesion capabilities of textile reinforcements in rubber using non-vulcanized material.

6 Project Assessment

6.1 Achieved goals

The goal of this thesis was to determine the best standard conditions to perform a dynamic test able to evaluate the adhesion performance between steel cord and rubber matrix and achieve results that match the tire's real conditions. For this study it was included two less time consuming test methods: The Dynamic t-test and the 3-Cord test.

Both the Dynamic t-test and the 3-Cord adhesion test revealed to be truly promising methods for further testing of the adhesion performance. They ensured to have the capacity of reproducing results similar to the drum-test, consuming less time and potential of testing future compound recipes.

6.2 Additional projects

Another goal of this study was to evaluate the use of different sample constructions and its effects on the final results when compared with the standard procedure. The Green adhesion study showed potential of evaluating the adhesion capabilities of textile reinforcements in non-vulcanized material, using different sample constructions.

6.3 Limitations and Future Work

The main limitation of these studies was the available time to perform, repeat and add more experiments to the studies. Due to the available time and equipment, it was not possible to test the standard conditions on any other material than the reference compound.

For a future investigation, the standard conditions should be tested on the proposed future compounds that incorporate different amounts of accelerators and no percentage of resorcinol. Other aspects for further studies would be the investigation of another testing technique to reduce/eliminate the friction between the sample and the clamp on the 3-Cord test, the combination of different aging conditions to provide the sample to get in touch with more service condition of the tire and the number of cycles influence on the dynamic t-test.

Regarding the Green adhesion test, more materials should be added to this study including materials with similar cord thickness and other rayon and nylon materials with different values of EPDM to try to achieve the same conclusions as PET.

6.4 Final Assessment

These studies required an intense initial gathering of information, regarding tire's reinforcements, different adhesion test methods and material property's changes during the aging and fatigue conditioning. It was quite changeling to get all the needed information to start the studies and this took a lot of access to the Continental's service system to provide books and articles.

The main difficulty for this thesis was to propose the set conditions for the different experiments and to manage the different test methods due to the lack of available time and equipments. Despite this, it's believed that I succeeded in these studies and had a positive performance throughout the company's view.

References

Almeida, V. M. (2012). *Characterization of the factors involved in hte tire production process.* Universidade do Minho.

Bekaert Combustion Technology BV. (2016). *Stell Cord.*

Brewer, D. H., Clark, P. S., & Gent, P. A. (February 2006). *The Pneumatic Tire.* Washington: U.S. Department of Transportation - National Highway Traffic Safety Administration.

Burghof, H. (2015). *Determination of "green adhesion" of cord fabric.* Hannover.

Chandra, A. K., & Mukhopadhyay, R. (1995). *Studies of Dynamic Adhesion Between Stell Cord and Rubber Using a New Testing Method.* India: Rubber Technology Center, Indian Institute of Technology.

Cinaralp, F., & Zullo, L. (2012). *Reinforcing Filtters in the Rubber Industry.* European Tyre and Rubber Manufacturers Association.

Continental AG. (April 2016). *Continental Corporation*. Von http://www.continental-corporation.com/www/portal_com_en/themes/continental/channel_facts_figures/facts.html abgerufen

Continental AG. (2008). *Tyre Basics Passenger Car Tyres.* Germany.

Crowther, B. (2001). *Handbook of rubber Bonding.* Shawbury: RAPRA Technology LTD.

Felten, T. (May 2016). *Task Force : Advanced Dynamic Adhesion Test Method.* Hannover: Continental AG.

Frampton, R. C. (2009). *The Dynamic Testing of Elastomers.* Technical Director Davenport-Nene Testing Systems.

Fulton, W. S. (2004). *Steel Tire Cord-Rubber Adhesion.* Manchester.

Guelho, I., Reis, L., & Fontul, M. (2012). *Complex Young Modulus For Rubbercork Composites.* Lisbon, Portugal: Institute of Materials and Surfaces Science and Engineering (ICEMS), Instituto Superior Técnico.

Hankook Tire. (2016). Abgerufen am April 2016 von Tire Structure: http://www.hankooktire.com/global/tires-services/tire-guide/tire-structure.html

Investigation on effects of dynamic fatigue frequency, temperature and number of cycles on the adhesion of rubber to steelcord by a new testing technique. (2013).

Jamshidi, M., Afshar, F., & Shamayeli, B. (2006). *Evaluation of cord/rubber adhesion by a new fatigue test method.*

K.Mitsuhashi. (1981). *Dynamic adhesion fatugue tests II.* Nippon Gomu Kyokaishi.

Kramer, T. (2015). *Basics of Reinforcements.* Hannover.

Louis, A., Noordermeer, J., Dierkes, W., & Blume, A. (2014). *Technologies for polymeric cord/Rubber adhesion in tire applications.* Enschede, The Netherlands: Faculty of Engineering Technology.

Mitsuhashi, K. (1981). *Methods of dynamic adhesion tests.* Nippon Gomu Kykaishi.

MTS System Corporation. (2006). *MTS 810 & 858 Material Testing Systems.* Eden Prairie.

NOKIAN TYRES PLC. (2008). *Reinforcing materials in rubber Products.* Ohio, U.S.A.

Omark, M. (2014). *Brush-model Simulation of Tire-Road Friction.* Luleå University of Technology.

REESA. (2016). *Technical Datasheet - Specific information for technical planners and painters.* Bremen.

Reuters. (May 2016). *Continental AG (CONG.DE)*. Von Reuters: http://www.reuters.com/finance/stocks/overview?symbol=CONG.DE abgerufen

Shi, X., Ma, M., Lian, C., & Zhu, D. (2013). *Investigation on effects of dynamic fatigue frequency, temperature and number of cycles on the adhesion of rubber to steelcord by a new testing technique.* China.

Zwick Roell. (April 2016). *AllroundLine - the perfect system for individual testing requirements and for all applications*. Von Zwick Roell: http://www.zwick.com/en/products/static-materials-testing-machines/testing-machines-from-5-kn-to-250-kn/allround-line-materials-testing-machines.html abgerufen

Appendix A – Sample preparation

Appendix A.1 – Green adhesion sample preparation

This test requires the preparation of 4 strips: 2 strips with dimensions 100 x 100 mm (A); 1 strip with dimensions 100 x 150 mm (B); 1 strip with dimensions 100 x 50 mm (C). The cut pieces are positioned as shown in figure A.1.

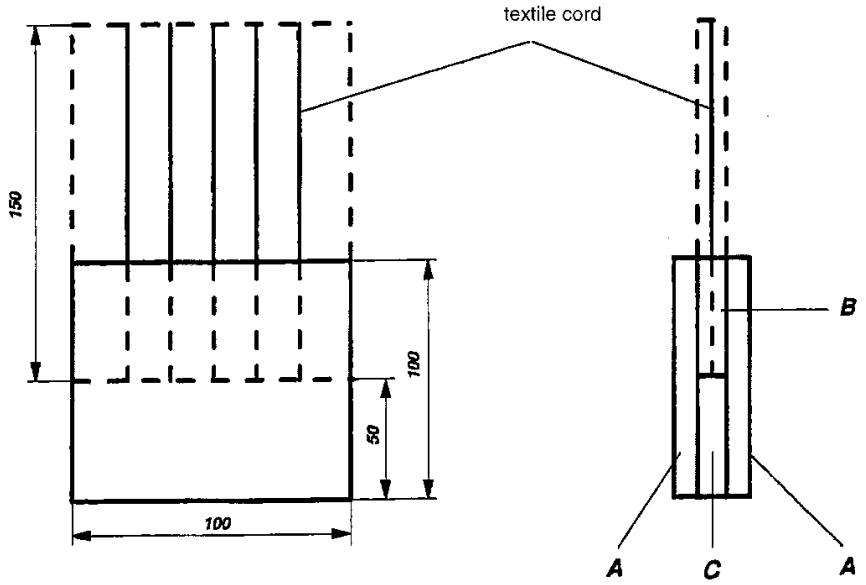

Figure A. 1 - Dimension of the strips and sample construction of the complete specimen (source: Burghof, 2015)

In one of the layers A is placed the strip C and above this one is placed the layers B. The layer B depends on the desired sample construction that can be calendered fabric, calendered cords or dipped cords as shown on the figure A.2.

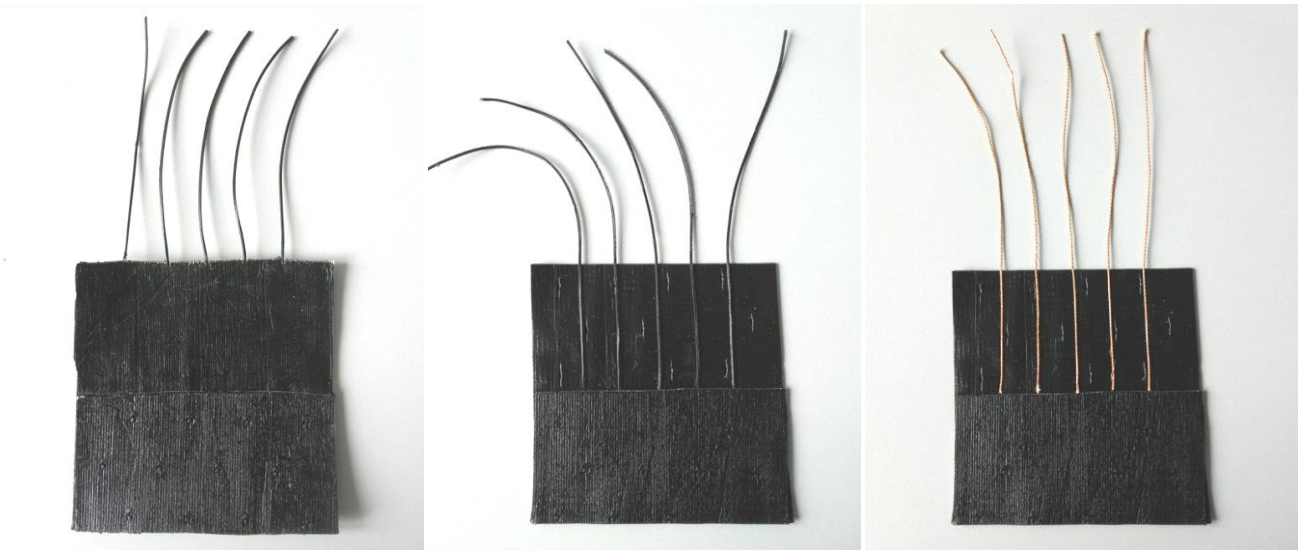

Figure A. 2 - Illustration of the different sample contractions: calendered fabric (left); calendered cords (middle); dipped cords (right)

The five textile cords in the test material section B that extends above the rest of the assembly (approximately 100 mm) are exposed for testing (the rubber on the cord is removed). The 5 cords should be a uniform distance apart, approximately 15mm, depending upon cord end count. The distance of the outer cords must be 20 mm from the edges. The remained layer A is then placed over the sample creating the final result as illustrated on figure A.3 (Burghof, 2015).

Figure A. 3 - Example of prepared sample for testing

Appendix A.2 – 3-Cord Adhesion sample preparation

This test uses two layers of standard rubber compound material with steel cords equally separated from each others. The sample has 26 cm of length, 10 cm of width and 1 cm of thickness. Before curing, 1 in each 3 cords is removed sequentially from one of the samples till it reaches 7.5 cm, and these can never be the cords on the edge of the sample.

From previous tests performed in the company, it was defined that the bottom layer must be prepared with a steel cord angle of 22 ºC (fig. A.4) due to high stiffness of the samples performed previously that limited the conditions used for the fatigue procedure.

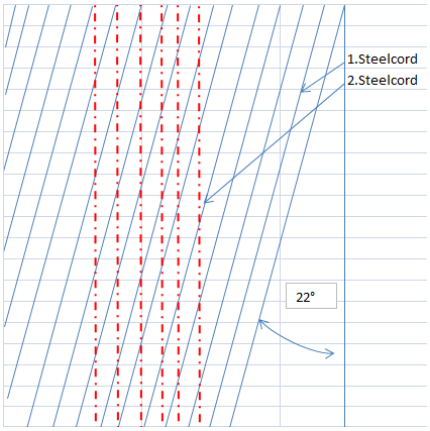

Figure A. 4 - Illustration of the angle formed by the to layers when combined together (source: Thomas Felten, 2016)

The layers are placed together and then go throw a curing procedure at 25 bars and 160 ºC during 30 minutes using the mould shown on figure A.5.

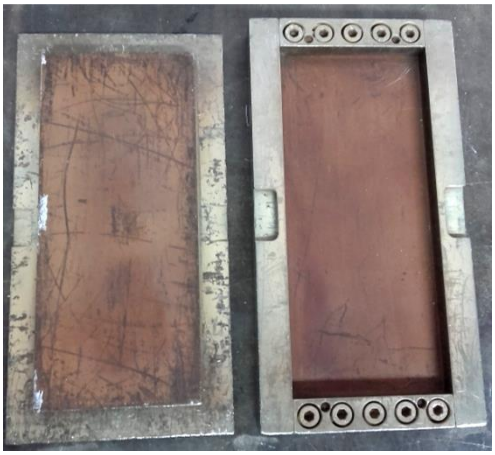

Figure A. 5 - Mould used to prepare the 3-Cord Adhesion samples

The result is shown on figure A.6, as well as the evaluation o the sample from after curing to after aging and last to fatigue.

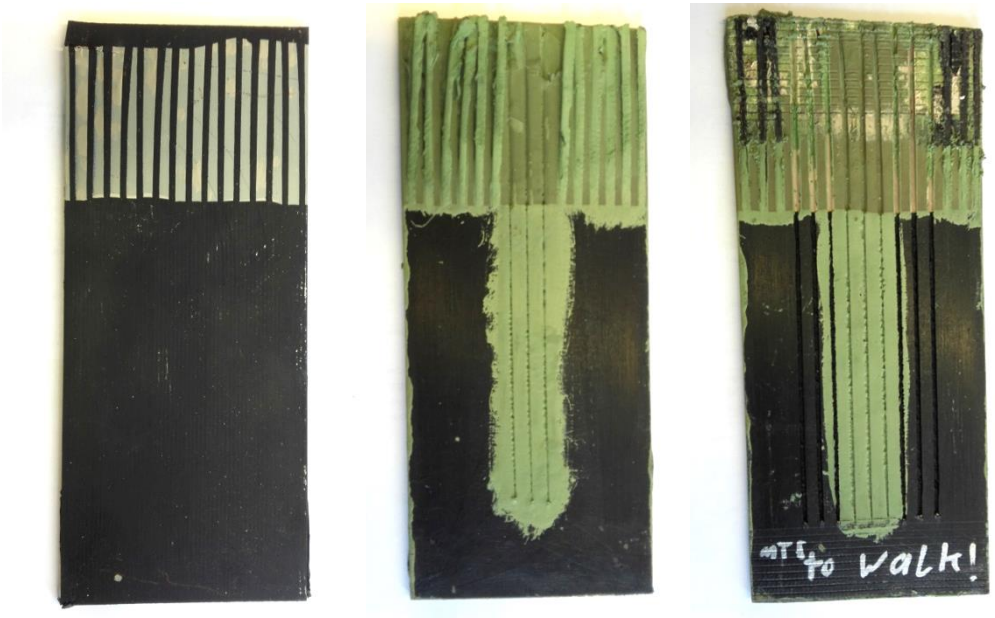

Figure A. 6 - 3-Cord Adhesion sample fresh (left); after aging condition (middle); after fatigue (right)

Appendix A.3 – Dynamic T-Test sample preparation

The standard t-test sample is characterized by a single row of rubber with 10 cords embedded. For this, it's needed 2 layers with 4 mm of thick rubber compound and MBL Steel Cord.

The first layer is place on the mould (fig. A.7) and then the cords are placed on the top and after the other layer. The mould must be pre-heated at a temperature of 150–170 °C for 30 min. The curing procedure after is performed at the same temperature for 30 minutes and the samples must rest for 3 hours before proceeding the test.

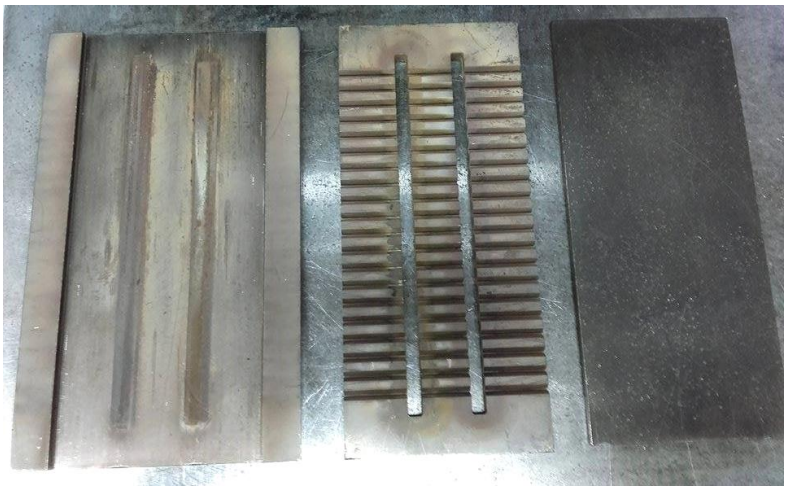

Figure A. 7 - Mould used to prepare the Dynamic T-Test samples

The result is shown on figure A.8, as well as the evaluation of the sample from fresh to after fatigue.

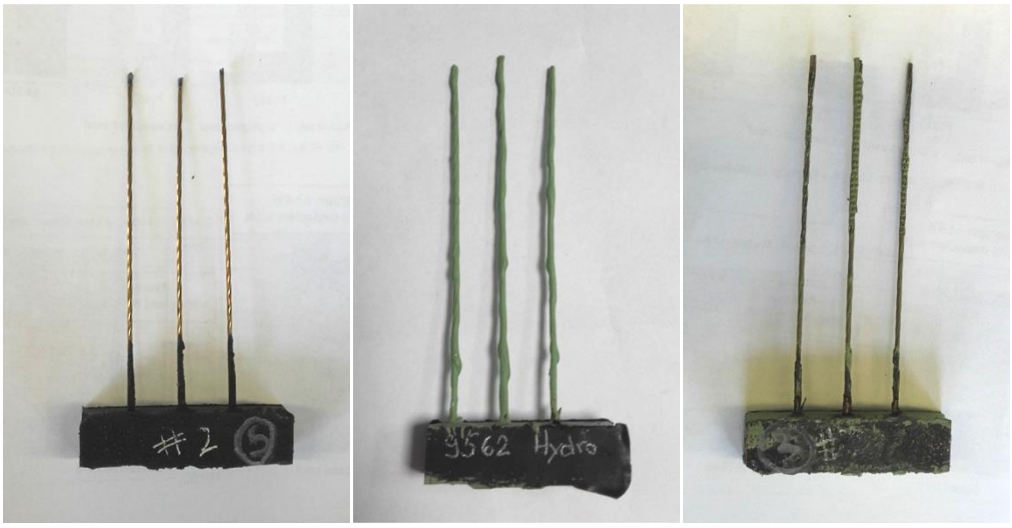

Figure A. 8 - Dynamic T-Test sample fresh (left); after aging condition (middle); after fatigue (right)

Appendix B – Lab test results

In this chapter is presented all the results from the tests performed for the textile and steel reinforcement studies.

Appendix B.1 – Green Adhesion Test

The results regarding the green adhesion test are presented on the table B.1.

Table B. 1 - Test results from the green adhesion test

Material	Green adhesion (N)		
	Standard test	Dipped cord	Calendered cord
N1204	29	11	21
		9	15
		11	18
		9	18
		12	22
P1319	39	16	26
		15	24
		13	32
		13	32
		14	22
P1457	59	22	41
		16	37
		15	42
		19	36
		19	36
R3002	84	37	61
		33	55
		46	58
		30	49
		36	55

Appendix B.2 – 3-Cord Adhesion Test

The results regarding the 3-Cord Adhesion test are presented on the Appendix B.2.1, B.2.2, B.2.3 and B.2.4, depending on focus study of the study.

Appendix B.2.1 – Influence of the Sample's thickness

In this chapter is presented all the results from the study of the influence of the sample's thickness on the test results. On the table B.2 is shown the sample's thickness all over the sample's strain and on the figures B.1 and B.2 it's shown the test results and the modified test results, respectively.

Table B. 2 - Thickness's values measured on different points of the sample

Strain (mm)	Thickness (mm)	
	Left side	Right side
0	3.45	3.53
40	3.51	3.52
80	3.63	3.61
120	3.47	3.54
160	3.48	3.52
200	3.56	3.54
240	3.48	3.5
280	3.52	3.48

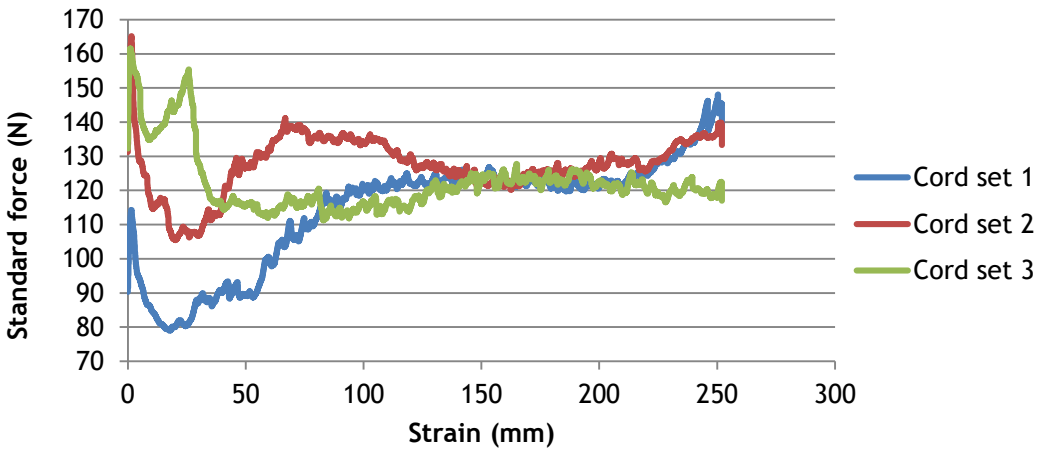

Figure B. 1 - Graphic representation of the test results

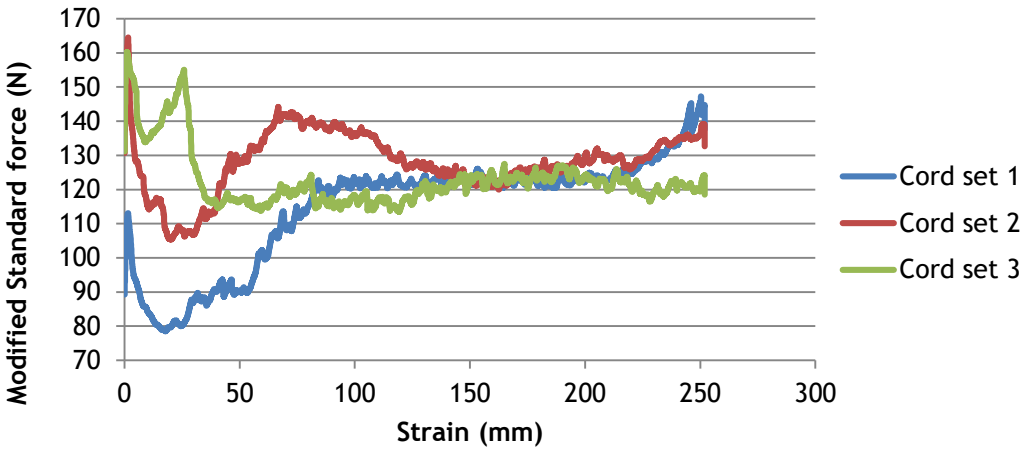

Figure B. 2 - Graphic representation of the modified test results

Appendix B.2.2 – Influence of the test starting position

In this chapter is presented all the results from the study of the influence of the test starting position (fig. B.3 – B.5)

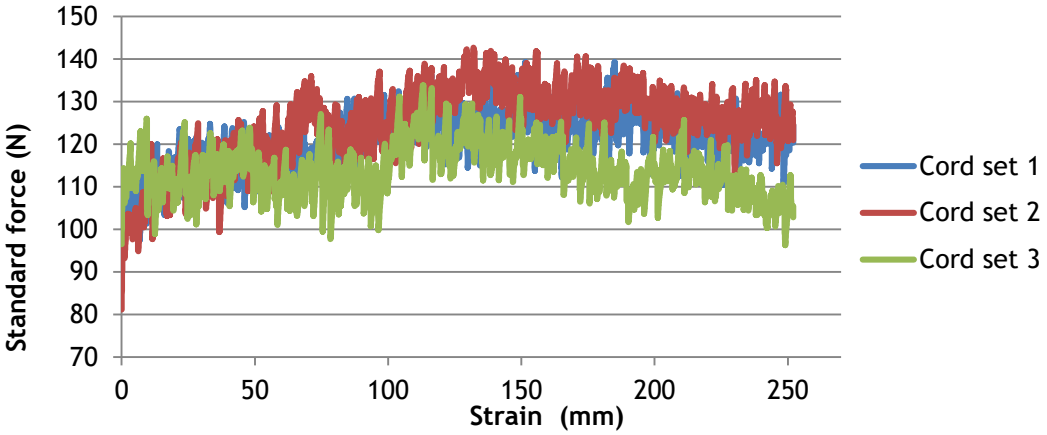

Figure B. 3 - Graphic representation of the standard force on the first test

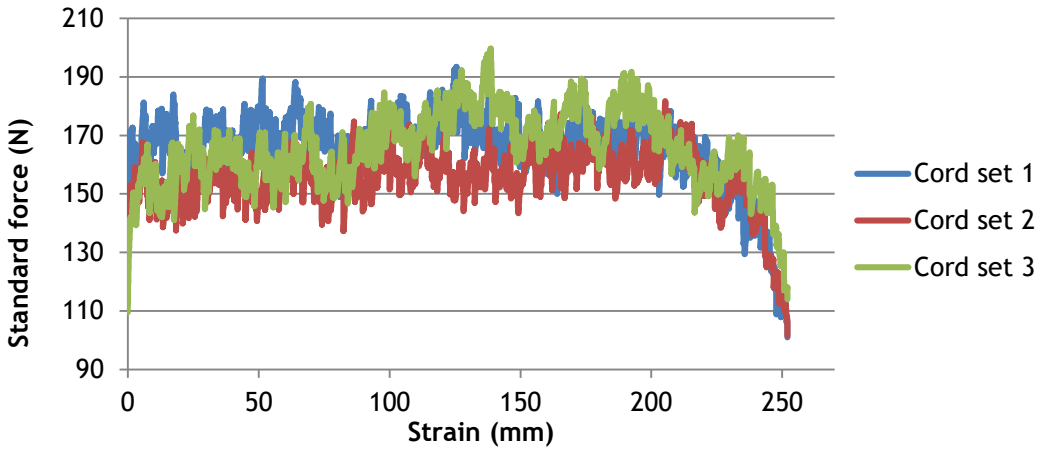

Figure B. 4 - Graphic representation of the standard force on the second test

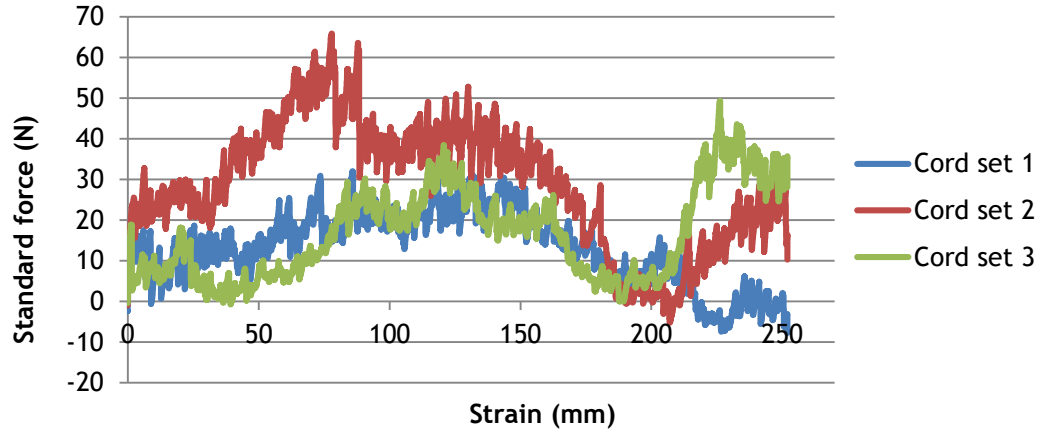

Figure B. 5 - Graphic representation of the standard force on the third test

Appendix B.2.3 – Reproducibility of the results

In this chapter is presented all the results from the study of the influence of the reproducibility of the test results (fig. B.6 – B.8).

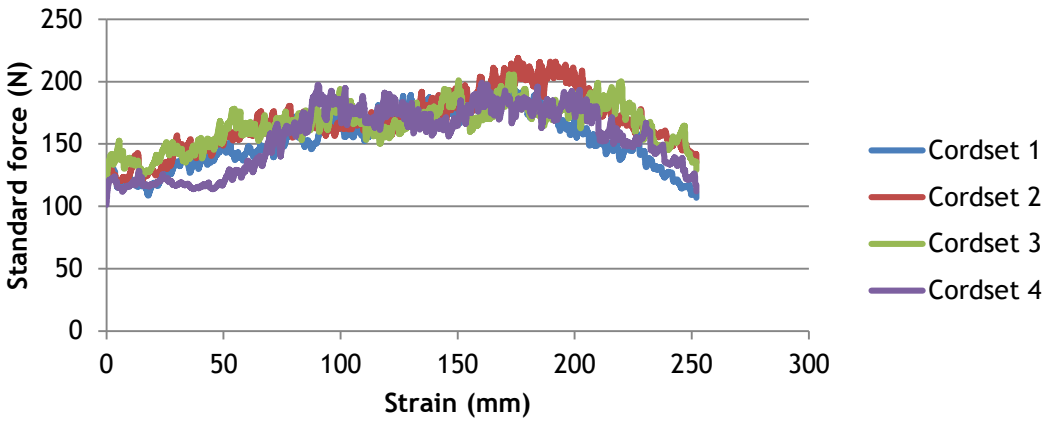

Figure B. 6 - Graphic representation of the standard force on the first sample

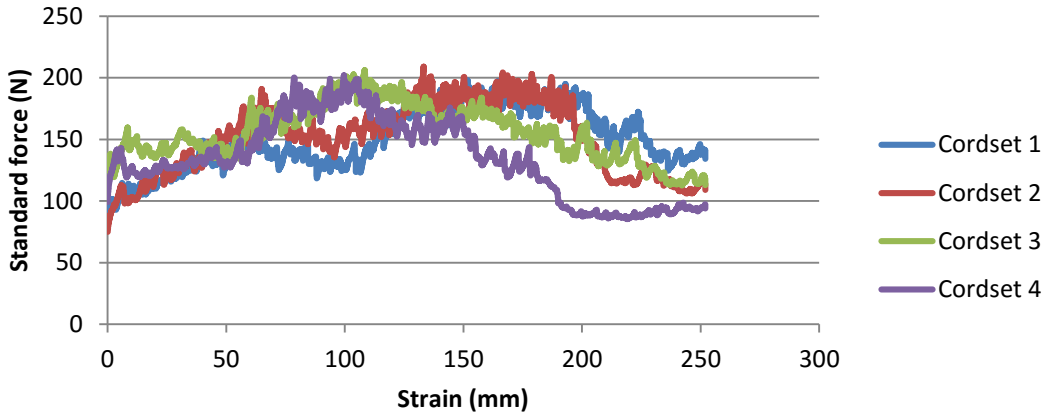

Figure B. 7 - Graphic representation of the standard force on the second sample

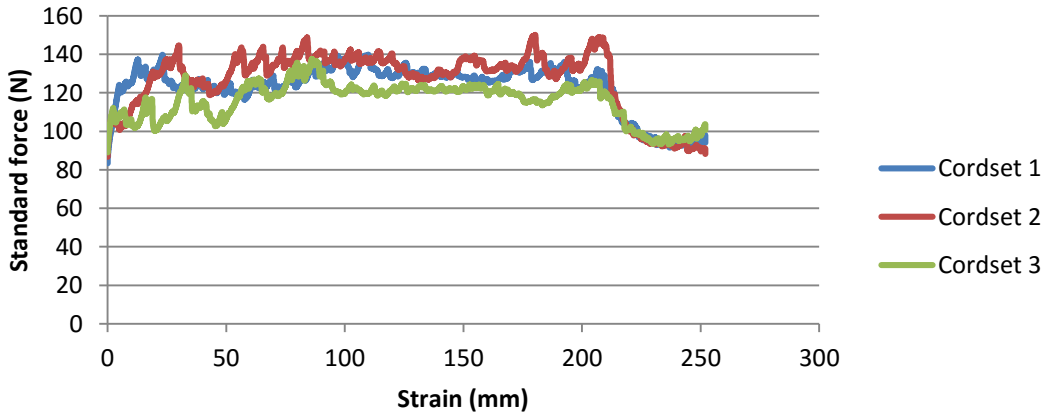

Figure B. 8 - Graphic representation of the standard force on the third sample

Appendix B.2.4 – Determine the best standard conditions

In this chapter is presented all the results from main test of the 3-Cord Adhesion Test, the determination of the best standard conditions (fig. B.9 – B.19).

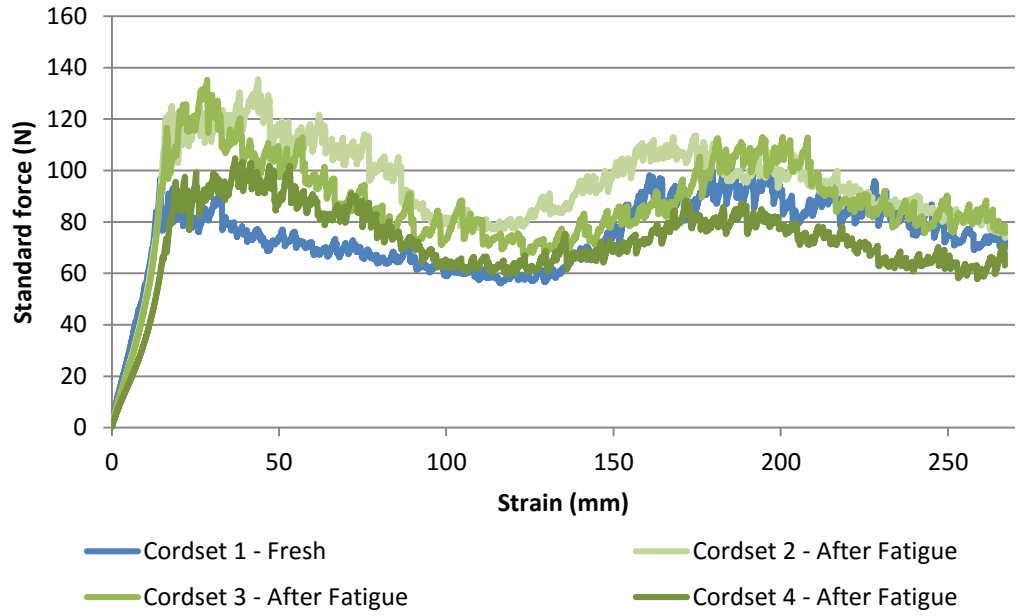

Figure B. 9 - Graphic representation of the standard force for the experiment 1

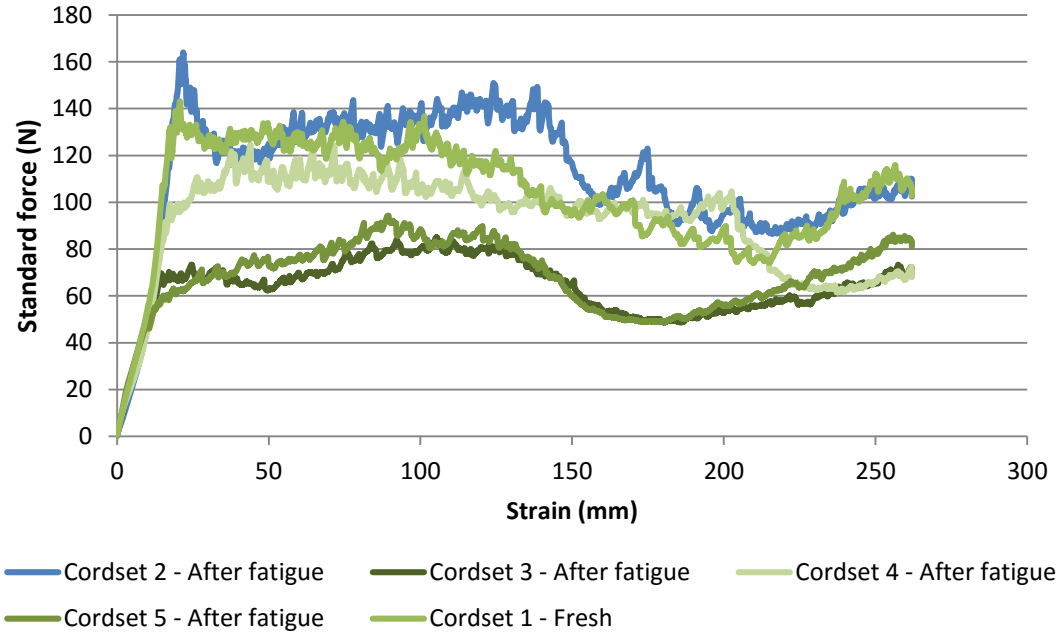

Figure B. 10 - Graphic representation of the standard force for the experiment 2

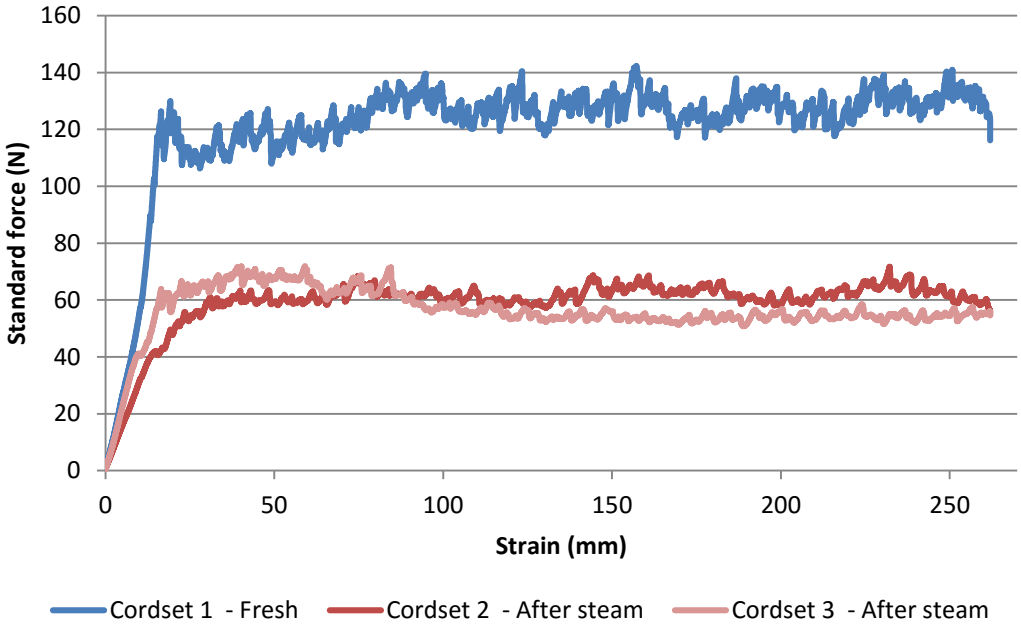

Figure B. 11 - Graphic representation of the standard force for the experiment 3

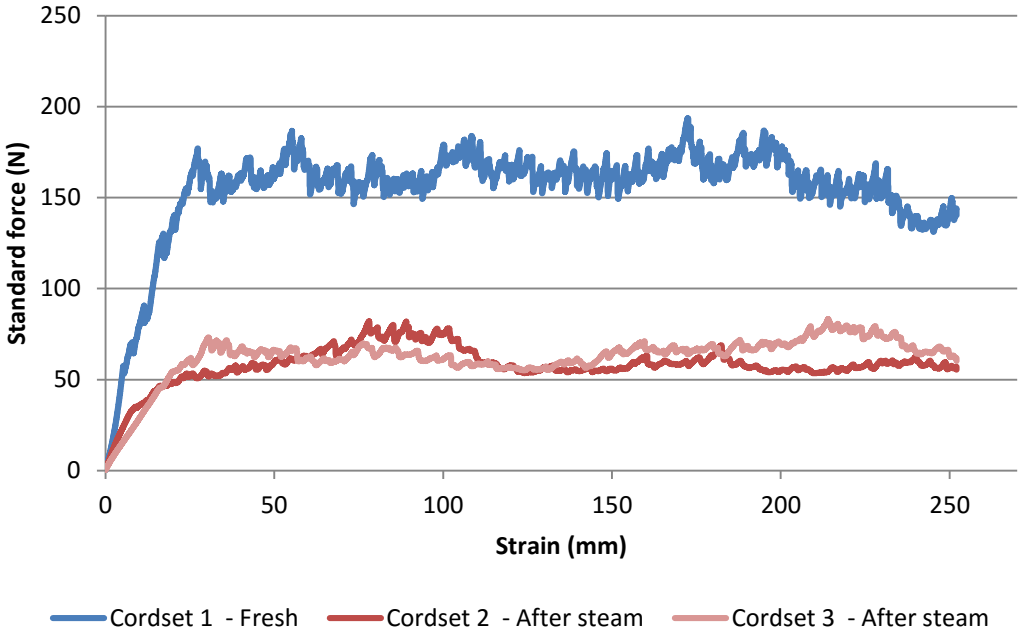

Figure B. 12 - Graphic representation of the standard force for the experiment 4

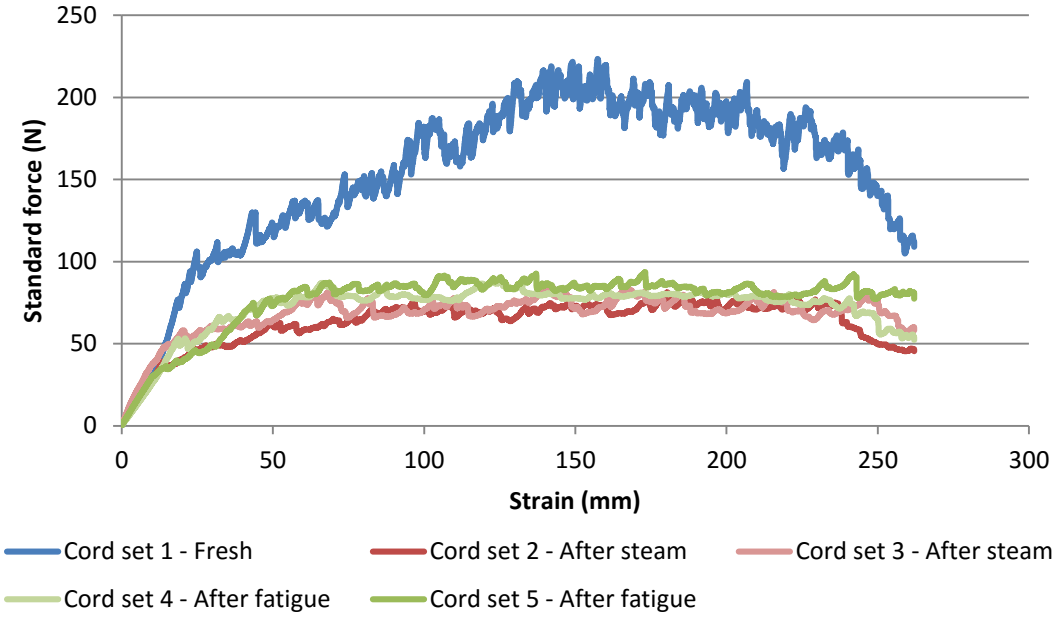

Figure B. 13 - Graphic representation of the standard force for the experiment 5

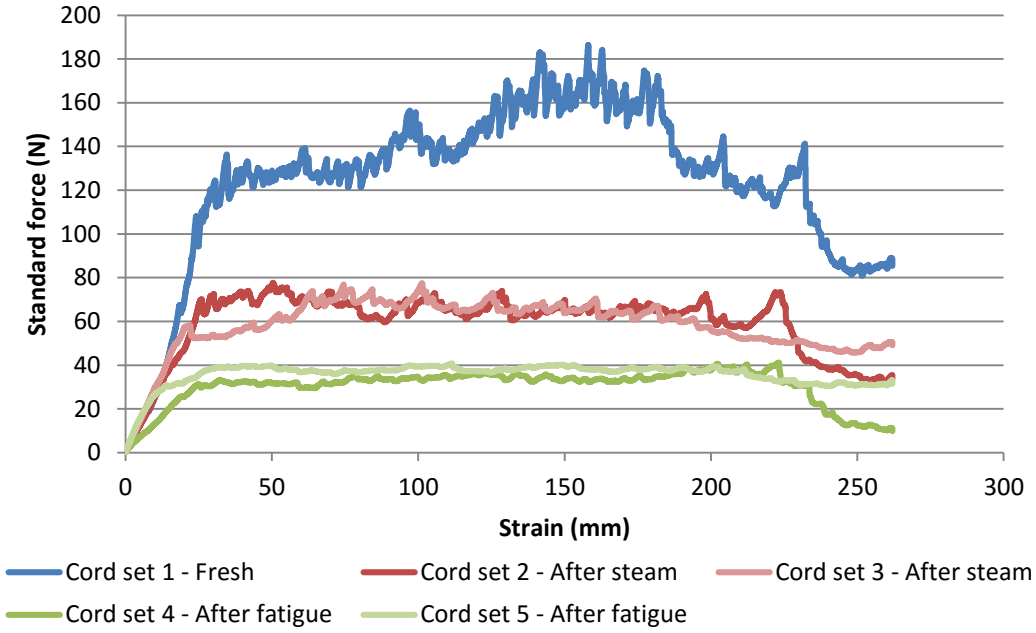

Figure B. 14 - Graphic representation of the standard force for the experiment 6

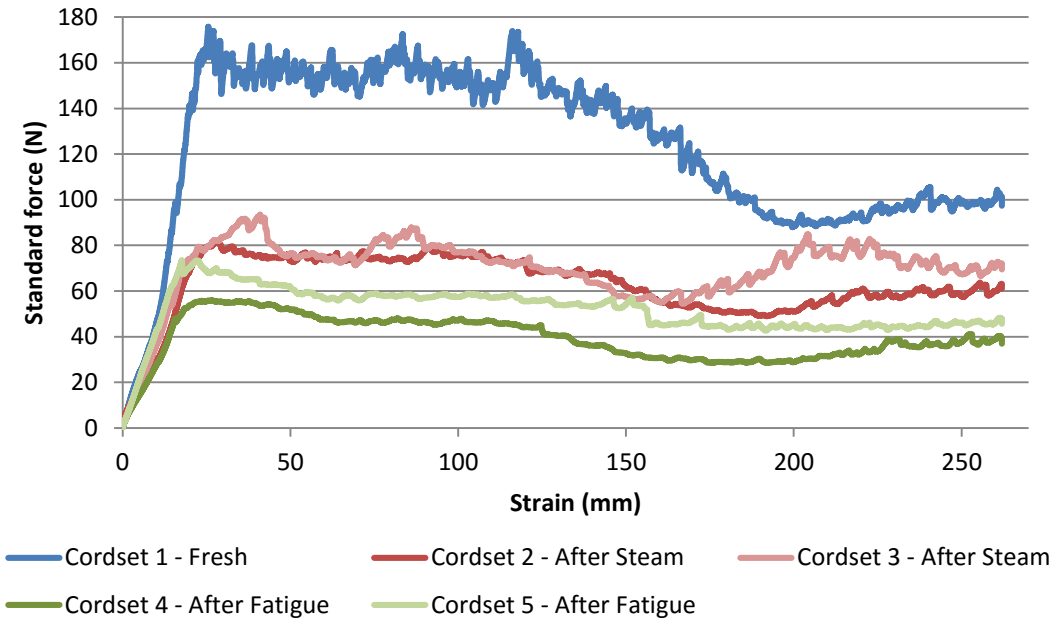

Figure B. 15 - Graphic representation of the standard force for the experiment 7

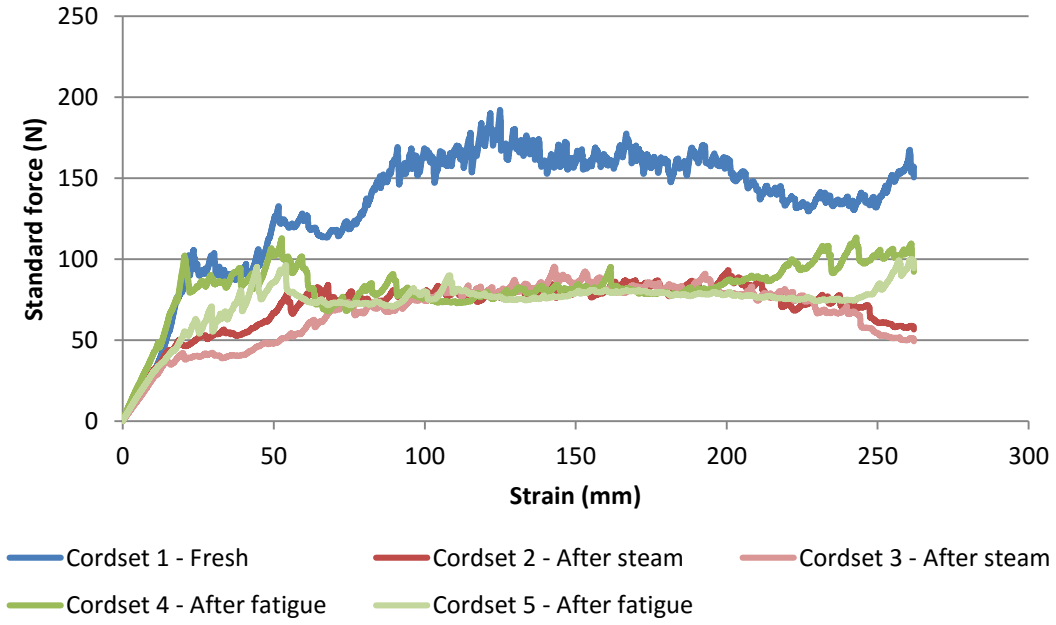

Figure B. 16 - Graphic representation of the standard force for the experiment 8

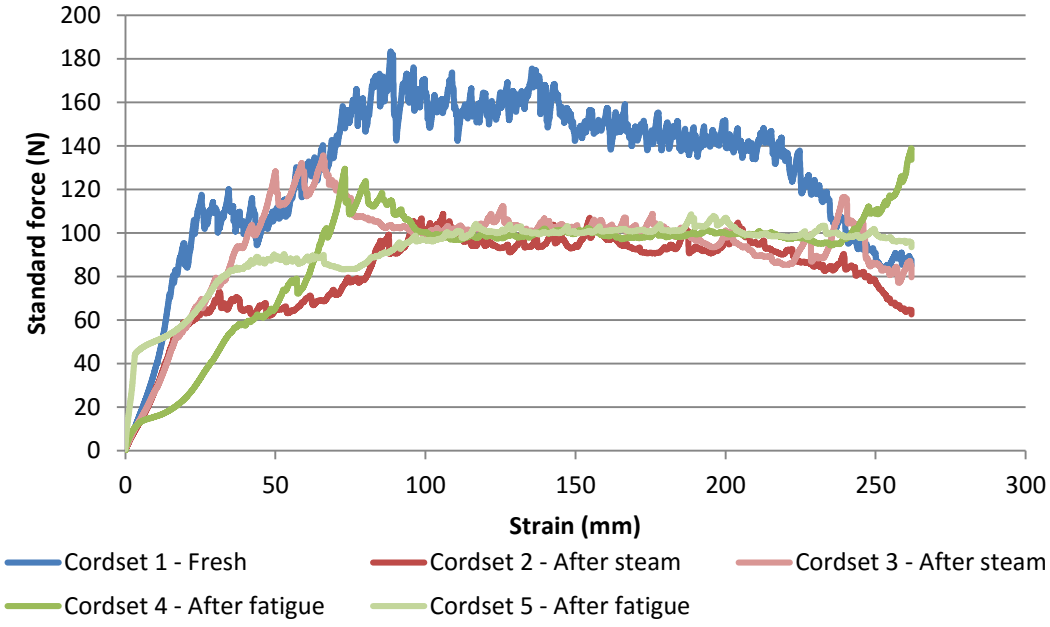

Figure B. 17 - Graphic representation of the standard force for the experiment 9

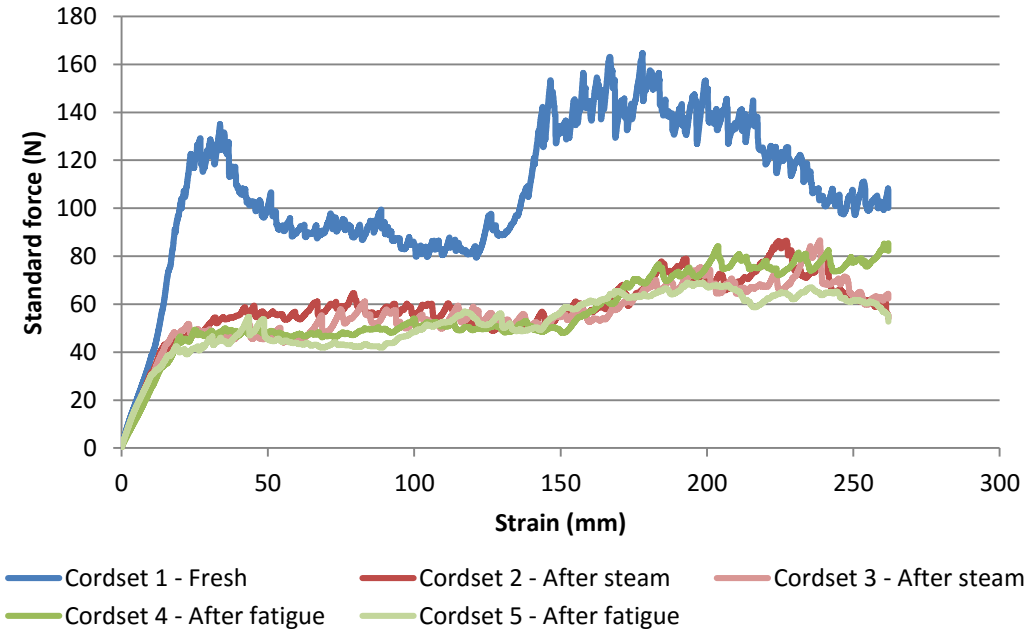

Figure B. 18 - Graphic representation of the standard force for the experiment 10

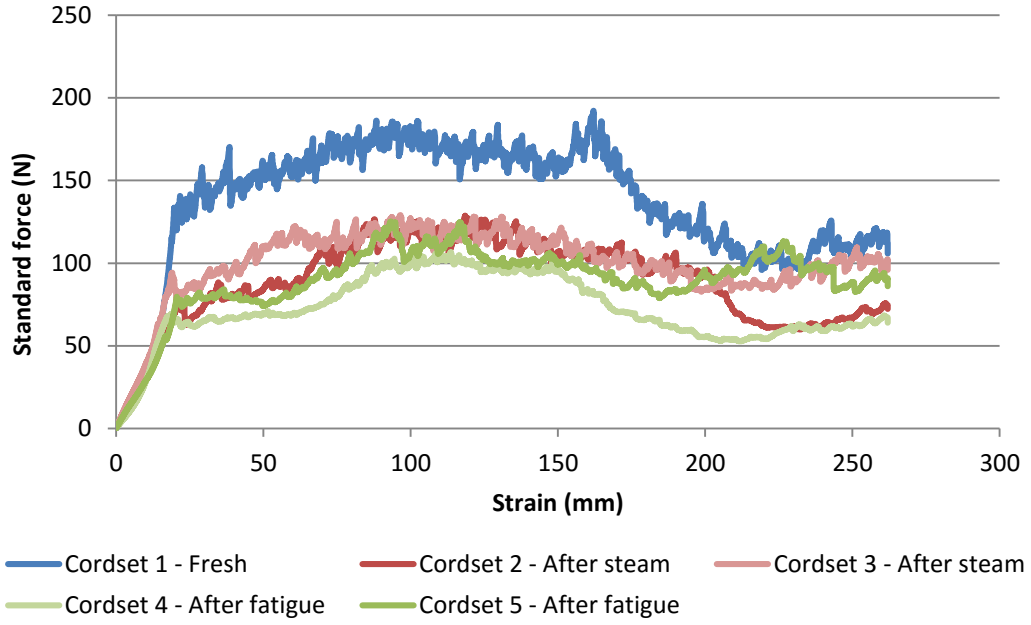

Figure B. 19 - Graphic representation of the standard force for the experiment 11

Appendix B.3 - Dynamic T-Test

The results regarding the Dynamic T-Test are presented on the figure B.20 and table B.3 and the evolution of the phase lag and complex dynamic stiffness on the figures B.21 and B.30.

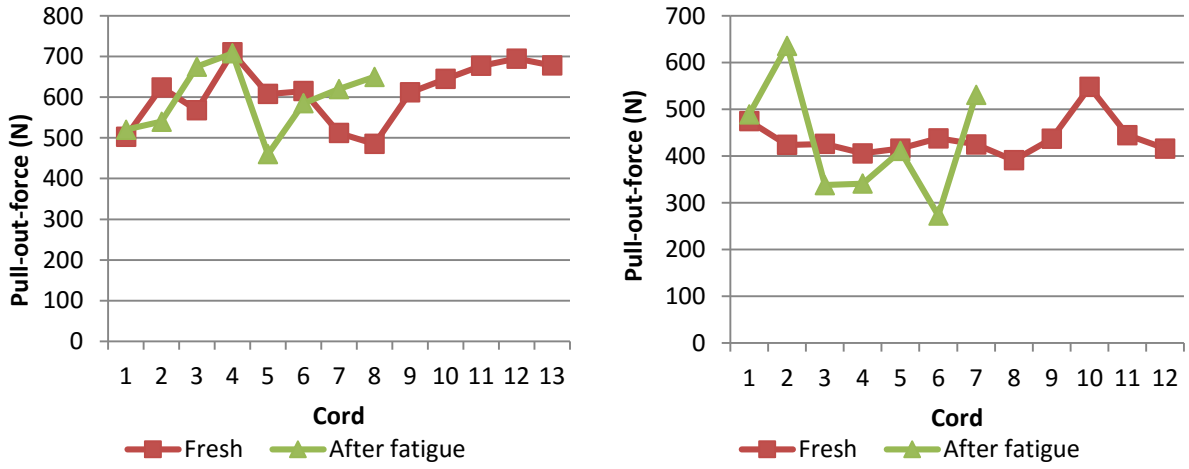

Figure B. 20 - Test results from previous tests (Experiment 1)

Table B. 3 - Test results from the dynamic t-test

	Cycles	Max Force (N)	K* (N/mm)	δ (°)
Fresh #1	22800	325.30	95.94	6.907
	26600	363.74	101.58	7.232
	23000	327.09	102.89	6.875
Fresh #2	28400	380.81	96.798	7.068
	22200	319.80	94.021	6.766
	23200	329.64	86.722	7.059
2 days under steam	19400	291.27	108.74	7.791
	19400	291.69	105.41	7.810
	19400	291.54	109.31	7.191
5 days under steam	16800	265.48	125.60	7.442
	13700	234.38	132.88	7.805
2 days under steam and fatigue on the Frank Machine	19800	295.60	113.99	6.956
	26400	361.08	115.53	7.567
	12800	226.21	100.74	7.278
5 days under steam and fatigue on the Frank Machine	17200	269.70	108.04	7.958
	19200	289.68	117.07	7.866
	13000	227.86	121.06	7.877
No aging condition and fatigue on the MTS Machine	16400	261.62	95.376	6.172
	17600	273.92	105.79	6.291
	21600	313.07	99.60	6.894
2 days under steam and fatigue on the MTS Machine	14600	243.72	131.67	7.127
	14200	238.98	115.65	7.959
5 days under steam and fatigue on the MTS Machine	10600	203.84	119.52	7.781
	10000	197.68	122.63	8.424
	7400	172.03	125.25	7.804

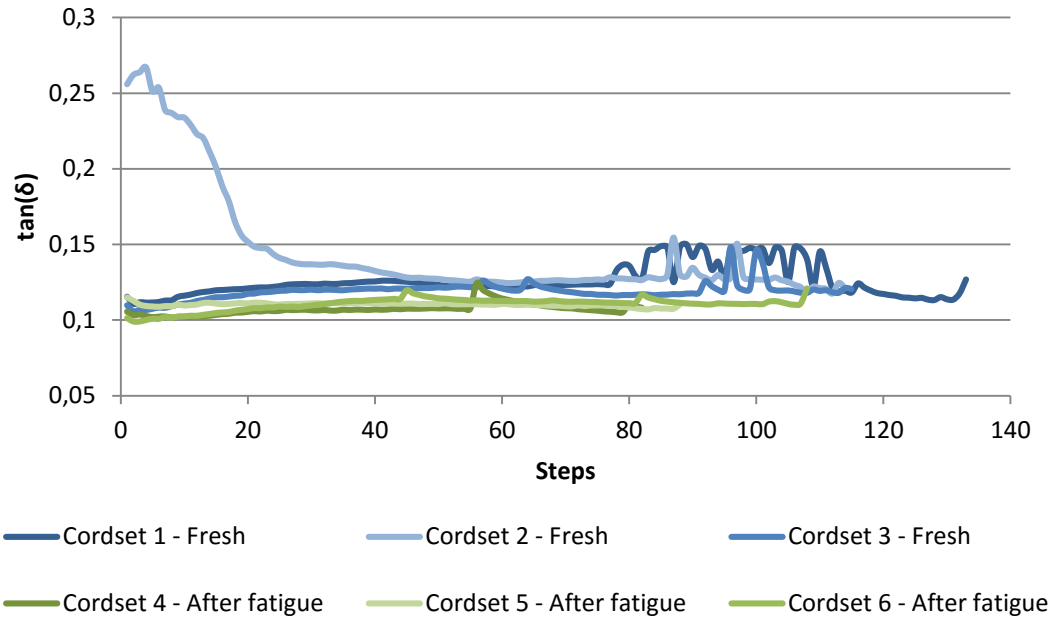

Figure B. 21 - Graphic illustration of the tan(δ) on the experiment 2

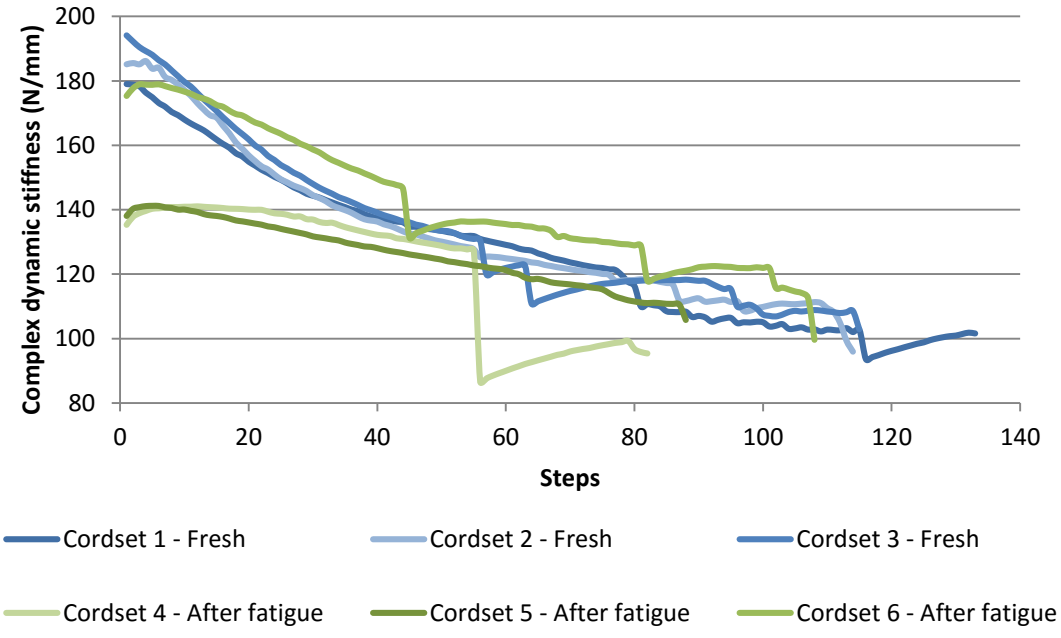

Figure B. 22 - Graphic illustration of the complex dynamic stiffness on the experiment 2

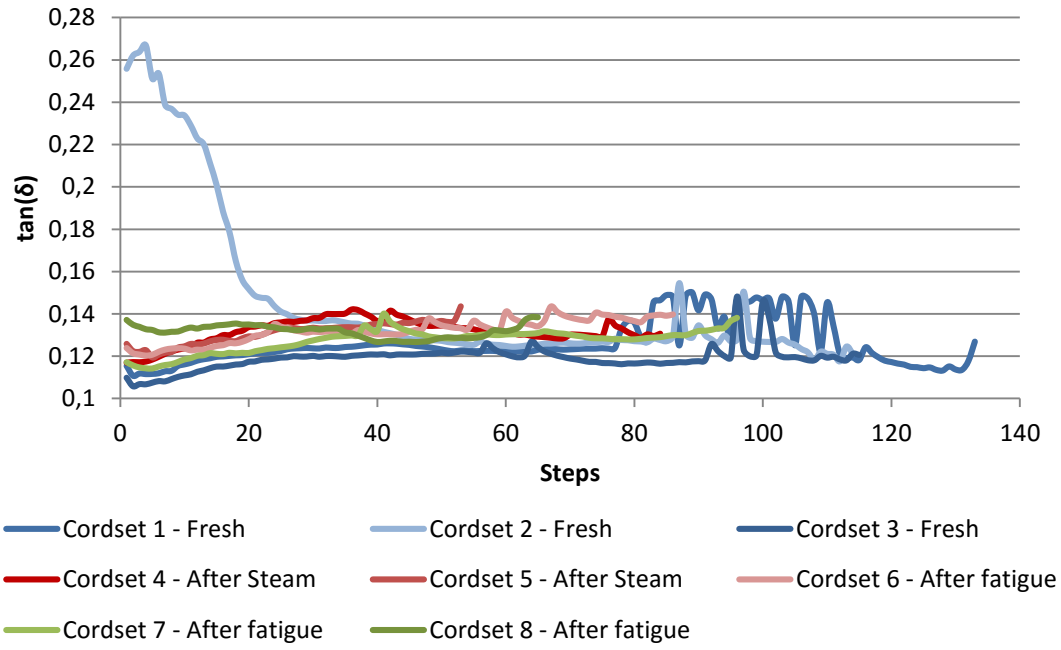

Figure B. 23 - Graphic illustration of the tan(δ) on the experiment 3

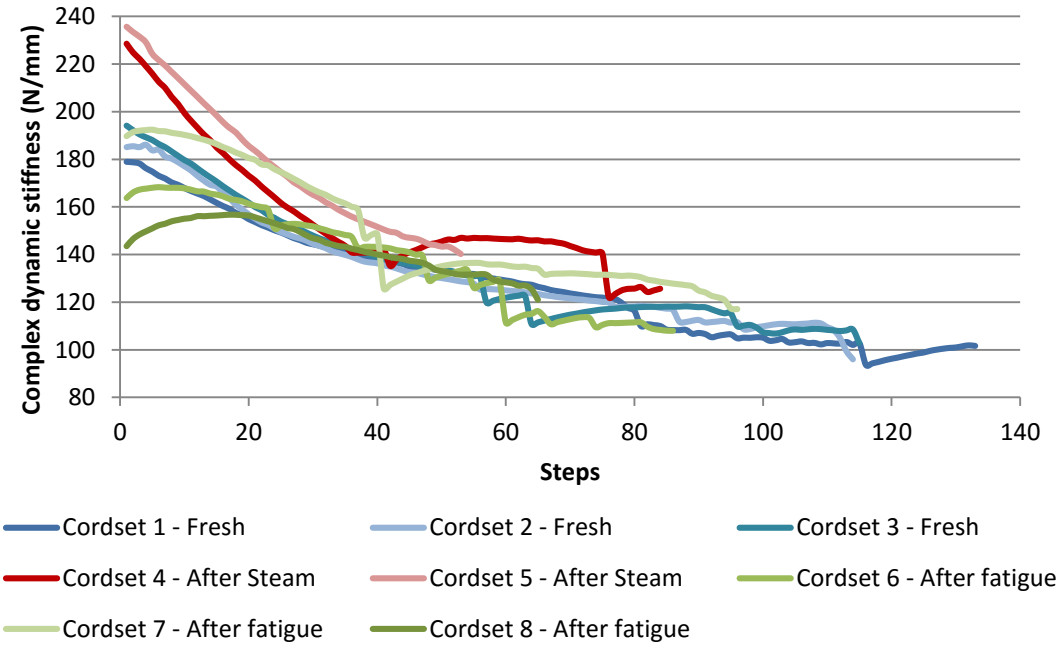

Figure B. 24 - Graphic illustration of the complex dynamic stiffness on the experiment 3

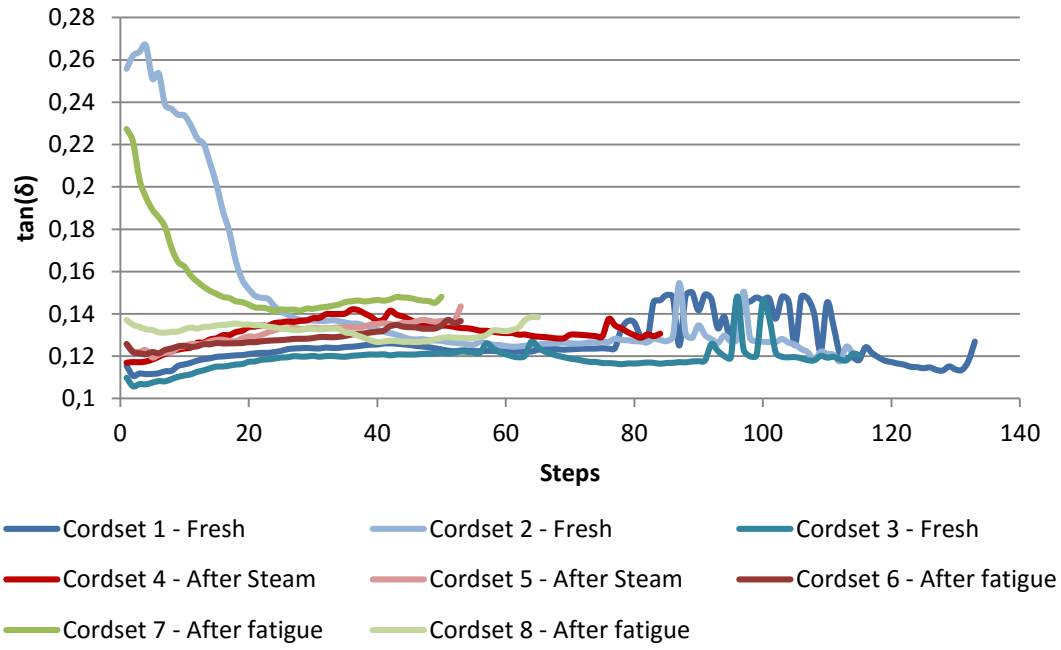

Figure B. 25 - Graphic illustration of the tan(δ) on the experiment 4

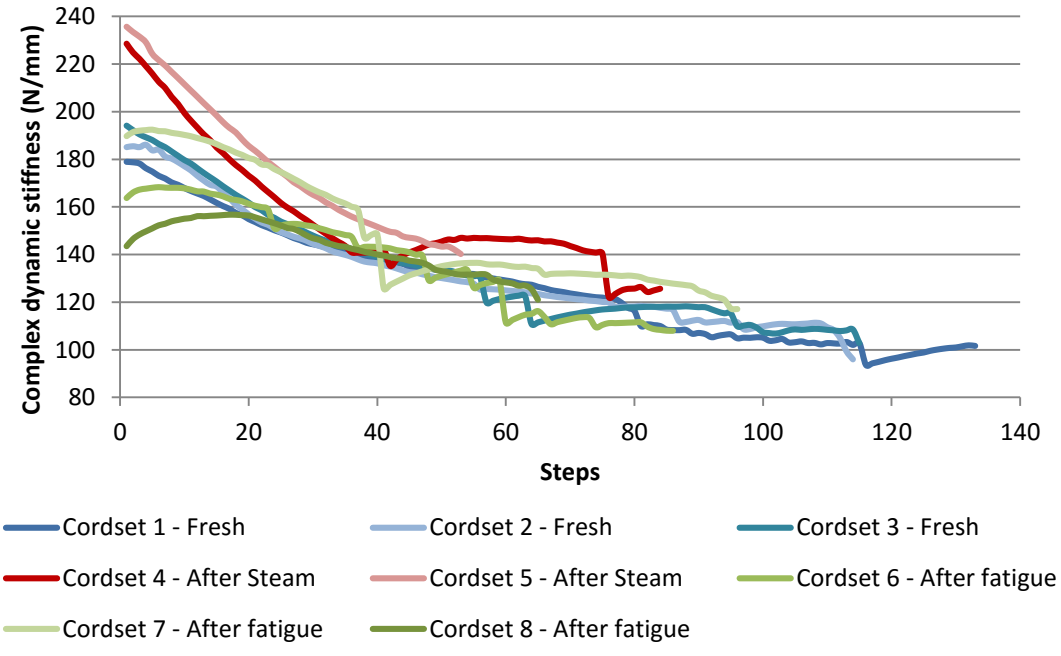

Figure B. 26 - Graphic illustration of the complex dynamic stiffness on the experiment 4

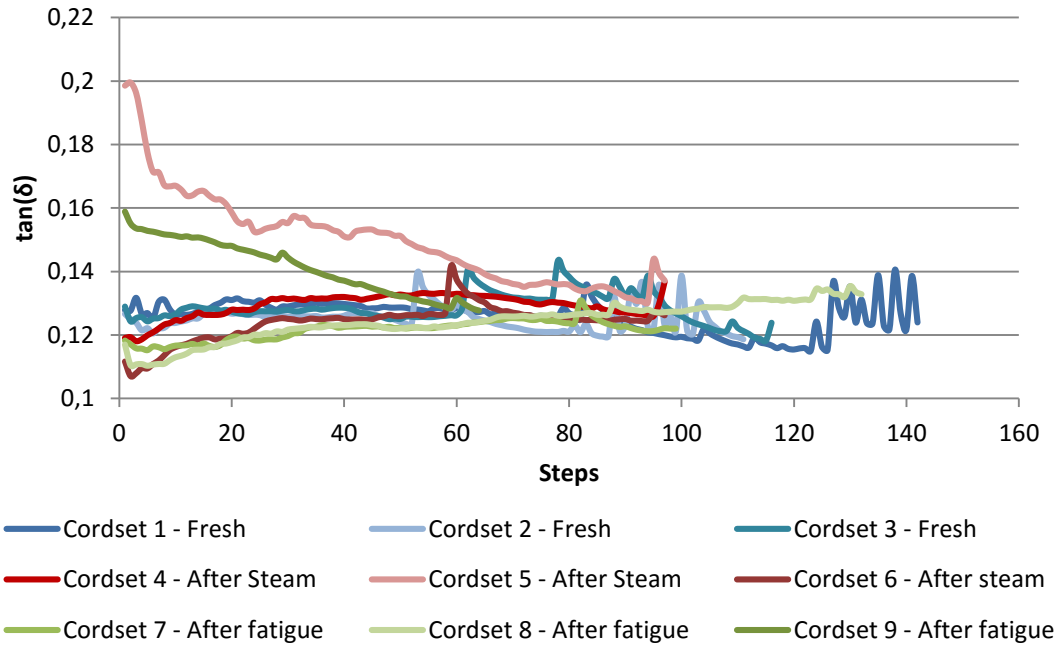

Figure B. 27 - Graphic illustration of the tan(δ) on the experiment 5

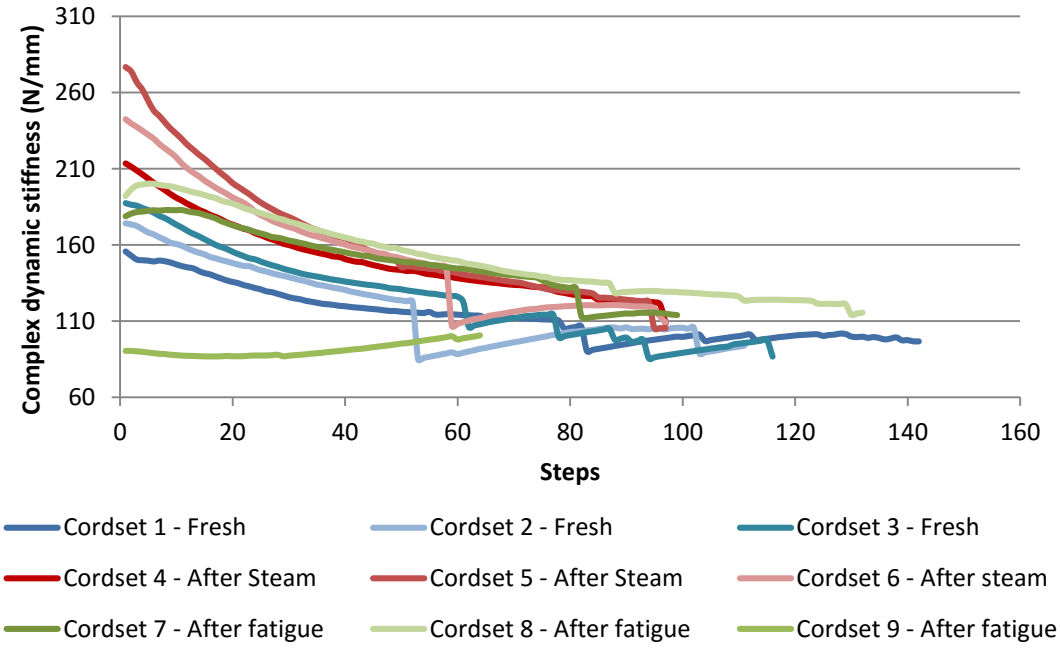

Figure B. 28 - Graphic illustration of the complex dynamic stiffness on the experiment 5

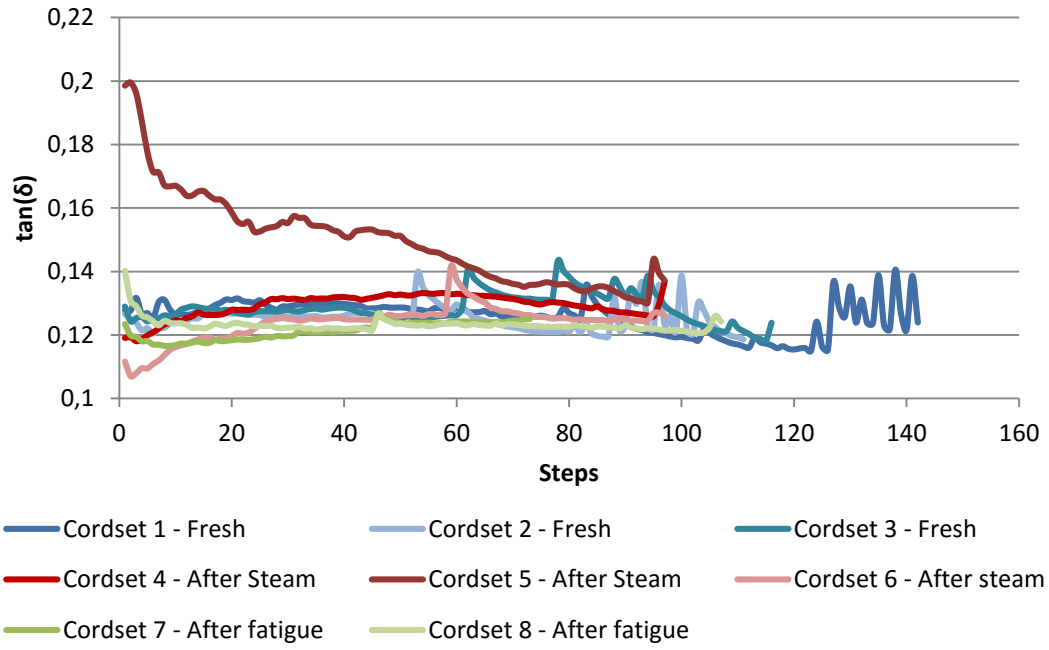

Figure B. 29 - Graphic illustration of the tan(δ) on the experiment 6

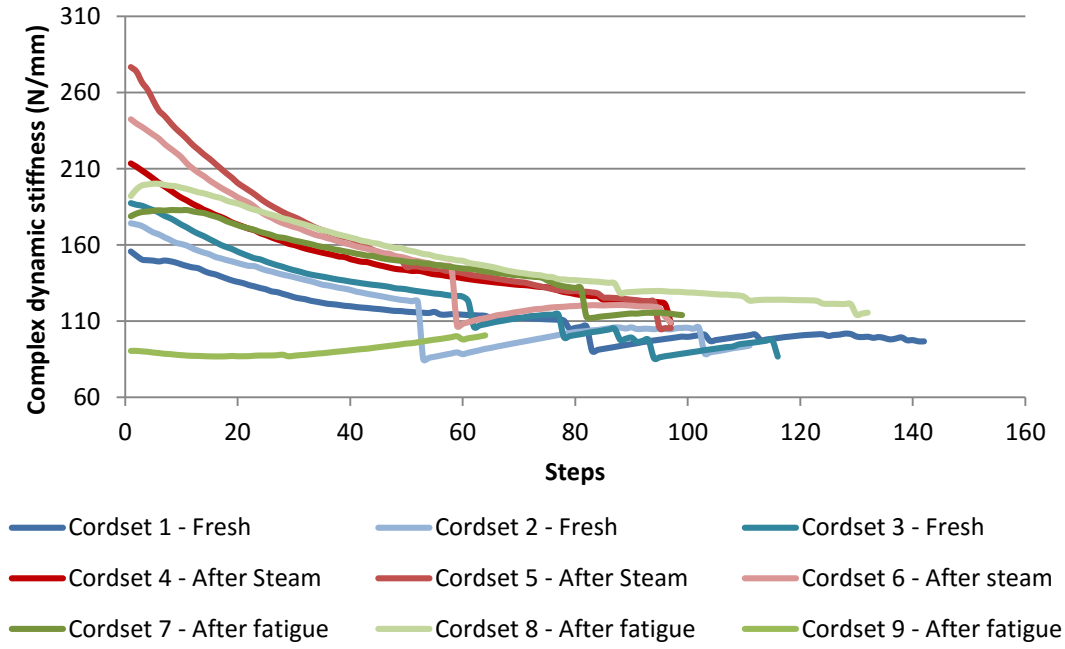

Figure B. 30 - Graphic illustration of the complex dynamic stiffness on the experiment 6